

1 **MERRA-based trend analysis identifies complex,**
2 **multidecadal patterns of changing climatic suitability**
3 **for Cassin's Sparrow (*Peucaea cassinii*)**

4
5 John L. Schnase^{1,2}, Mark L. Carroll¹,
6 Paul M. Montesano^{1,2}, and Virginia A. Seamster³

7
8 ¹ NASA Goddard Space Flight Center, Greenbelt, Maryland, 20708 USA

9 ² ADNET Systems, Inc., Bethesda, Maryland, 20817 USA

10 ³ New Mexico Department of Game and Fish, Santa Fe, New Mexico, 87507 USA

11
12
13
14
15
16
17
18
19
20
21
22 Corresponding author:

23 Email: john.l.schnase@nasa.gov

24
25
26 Author contributions:

27 JLS: Conceptualization, Formal analysis, Investigation, Methodology, Software,
28 Writing – original draft. MLC: Conceptualization, Formal analysis, Methodology, Writing –
29 review & editing. PMM, VAS: Formal analysis, Writing – review & editing.

30 Abstract

31 Cassin's Sparrow (*Peucaea cassinii*) is a grassland resident of the American Southwest.
32 Despite decades of study, there remains uncertainty regarding the conservation status of the
33 species. The species' past response to a changing climate may help explain this uncertainty,
34 especially if patterns vary across the species' range. In this study, we combine data from NASA's
35 Modern-Era Reanalysis for Research and Applications, Version 2 (MERRA-2; M2) with field
36 observations spanning the past 40 years to examine historical changes in climatic suitability for
37 Cassin's Sparrow across its full annual range within the continental United States. We examine
38 two time- and variable-specific time series using MaxEnt. The M2 times series uses a mix of 30
39 microclimatic variables and ecosystem functional attributes related to energy and water fluxes
40 for predictors; the MERRAclim (MC) time series uses 19 MERRA-2-derived bioclimatic
41 variables for predictors. Trend analysis reveals complex patterns of slowly increasing climatic
42 suitability over 69.5% of the study area in the MC time series accompanied by decreases over
43 24.4% of the area. Shifts in the study area-wide, weighted centroid for climatic suitability show a
44 northwesterly, 40-year displacement of 1.85 km/yr. The M2 time series points to a less favorable
45 history with increasing and decreasing trends over 54.9% and 40.1% of the study area,
46 respectively, and a westerly weighted centroid shift of 2.60 km/yr. A clear subset of seven M2
47 and MC variables emerged as the most important determinants of suitability over the past 40
48 years. These variables also demonstrated complex patterns of non-constant trends across the
49 study area. Suitability trends in both time series appear to have little in common with current,
50 state-level, abundance-derived conservation status assessments. Increasing winds, drying land
51 surface conditions, and variability in North American Monsoon rainfall appear to be dominating,
52 climate-related influences on the species. We thus see complex patterns of historical change in

53 climatic suitability depending on whether time series models are driven by bioclimatic variables
54 alone or by variables more aligned with ecological function. This leads us to conclude that
55 modeled estimates of climatic suitability for Cassin's Sparrow can vary widely depending on the
56 temporal frame, spatial extent, and environmental drivers considered, and that this variability
57 mirrors the uncertainty in the literature regarding the species' conservation status. Furthermore,
58 these factors should be taken into account in future conservation assessments for the species, and
59 retrospective ecological niche modeling, as applied here, offers a promising approach to
60 addressing these issues.

61

62 **Introduction**

63 Cassin's Sparrow (*Peucaea cassinii* Woodhouse, 1852) is an elusive, ground-dwelling
64 endemic of the arid grasslands of the southwestern United States (U.S.) and northern Mexico [1–
65 3]. Like many grassland birds, evidence gathered over the past several decades suggests that
66 Cassin's Sparrow is experiencing a contraction of viable habitat and declining regional
67 populations [4–8]. This is reflected in documents such as the State Wildlife Action Plan for New
68 Mexico, which lists Cassin's Sparrow as a declining species, susceptible to shifting
69 environmental conditions or disease outbreaks that could lead to rapid population changes [9].
70 However, other sources report the species as stable [10–13]. Partners in Flight identifies Cassin's
71 Sparrow as a species of low conservation concern [14], and, of nine grassland birds in New
72 Mexico, recent work has shown Cassin's Sparrow to be the only species for which gains in
73 suitable habitat are projected over the next 50 years [15]. NatureServe's assessment is more
74 complex, reporting Cassin's Sparrow to be imperiled in Oklahoma, vulnerable in Kansas and

75 Nebraska, and apparently secure in Texas, New Mexico, Arizona, and Colorado, while assigning
76 the species a global ranking of demonstrably secure [16].

77 These differing views likely arise, in part, from natural history traits that complicate the
78 observational record [3,5,17,18]. Cassin's Sparrow is a grassland-shrub specialist [19]. A
79 vegetation mix of grasses and low shrubs appears to be critical to the bird's breeding ecology;
80 however, considerable variation in the proportions of that mix seems to be well tolerated
81 [2,3,5,19]. Cassin's Sparrow also appears to be highly sensitive to precipitation, following the
82 movement of monsoon rains throughout the breeding season in an itinerant pattern that is
83 difficult to track or interpret [3,5,20]. Sorting out key ecological details, such as these, has been
84 complicated by the species' ground-dwelling habit. Often described as secretive, this non-
85 descript sparrow lives much of its life on the ground, nearly invisible to even the most
86 experienced observer, until the breeding season when males perform a flight display [2,3,5,21].
87 Males use this uncommon skylarking behavior to establish breeding territories, attract females,
88 and maintain pair bonds. Launching from an exposed perch atop a low shrub, birds fly 10 m or
89 more into the air, then flutter their wings in a slow descent to the ground or nearby perch while
90 producing their distinctive, primary song [2].

91 A better understanding of the temporal dynamics of Cassin's Sparrow's historical
92 response to a changing climate could help explain some of the uncertainties regarding the
93 species' conservation status and aspects of the species' natural history and ecology that may be
94 confounding the issue. We now understand that the multidimensional niche space of a species
95 may shift, through adaptation or acclimation, as may its demography in response to climate
96 changes [22]. We also know that climate change can drive shifts in the spatial distribution of
97 many bird species as they track suitable conditions. These shifts are the consequence of multiple

98 processes, including changes in habitat and the distribution of resources, dispersal patterns, and
99 carrying capacity [23]. While climate-based ecological niche modeling (ENM) is commonly
100 used to project anticipated responses by a species to a changing climate, less consideration has
101 been given to retrospective patterns of change that could, in some cases, shed light on the present
102 and future status of a species [24].

103 In this study, we combine data from NASA's Modern-Era Reanalysis for Research and
104 Applications, Version 2 (MERRA-2; M2) with field observations spanning the past 40 years to
105 perform a retrospective ENM analysis of Cassin's Sparrow's evolving environmental niche. In
106 doing so, we assume that a combined look at historical patterns of change in suitable conditions
107 alongside historical trends in the environmental drivers of those changes will provide new
108 insights into the ambiguities surrounding Cassin's Sparrow's status. Our approach focuses on
109 changes in climatic suitability and embodies a novel integration of three distinctive elements.

110 First, we base our analysis on environmental variables obtained solely from the M2
111 reanalysis. Climate reanalyses combine past observations with numerical models to generate a
112 consistent time series of hundreds of fundamental, physical drivers of the Earth system. They
113 offer a comprehensive description of Earth's observed climate as it has evolved over the past half
114 century at a fine temporal scale [25,26]. M2's information-rich, long-running, high temporal-
115 resolution data address ENM's growing requirement for ecologically-relevant environmental
116 predictors that can be tailored to specific modeling objectives while taking into account a
117 species' biological and ecological requirements [27–33].

118 The current study spans the 40-year period from 1980 to 2019 and is based on two
119 climatic variable time series. In one, we use 30 M2 variables selected to reflect key attributes of
120 the microclimate and climate-related ecosystem functioning [34,35]. The collection contains the

121 precursor temperature and precipitation variables from which the 19 classic, bioclimatic
122 predictors (i.e., bioclim variables) commonly used in ENM are derived [36,37]. In addition, it
123 includes environmental attributes of more direct biological significance that are not explicitly
124 represented in the 19 bioclim variables, such as soil moisture and evaporation from land, wind
125 direction and speed, and various solar radiation fluxes [36,38–42]. In the second time series, we
126 use 19 M2-derived bioclimatic variables modeled after the classic bioclim predictors [37,41].
127 Taken together, these two sets of predictors provide a more detailed view of macro- and
128 microclimatic factors influencing environmental suitability for different species than could be
129 realized by using the traditional bioclimatic predictors alone.

130 Our work with M2 variables complements a trend toward increased use of satellite-
131 derived ecosystem functional attributes (EFAs) to improve model performance in ENM-based
132 conservation practice [30,43–50]. In contrast to other types of predictors, EFAs, such as seasonal
133 heat dynamics, the net energy fluxes that drive trophic webs, primary productivity, vegetation
134 greenness, evapotranspiration, and soil moisture, relate to the performance of an ecosystem as a
135 whole, and their values are potentially the consequence of multiple ecosystem processes [49].
136 ENMs that explicitly incorporate EFAs enable a more integrative perspective on environmental
137 dynamics and allow for a more detailed characterization of the microclimatic conditions
138 experienced by a species [49,51–53]. As a source for ENM predictors in our work, climate
139 reanalyses provide a unique, readily-accessible mix of classic climatic variables and EFAs.

140 A second feature of the study is that we employ time-specific ENM in our analysis: our
141 dependent and independent variables are temporally aligned across the time-span of the study.
142 Detailed spatiotemporal information about the geographic distribution and changing dynamics of
143 climatic suitability for a species is critical to conservation planning [30,43–46,48,50,54–56].

144 ENM is often applied within a time-averaged framework in which the values of environmental
145 variables are averaged over time spans that are not in temporal registration with the occurrence
146 records upon which models are calibrated or tested [55,57]. While useful for exploring species
147 distributions at a broad level, modeling within a time-averaged framework can elide complex
148 effects of the environment on an organism, especially highly mobile or behaviorally complex
149 species [55,58–61]. Of particular concern to conservation work, studies have shown that
150 temporal mismatches in the time period spanned by occurrence data and the climate baseline can
151 decrease the utility and accuracy of ENM products [62–67].

152 In the current work, we use averaged values for our environmental variables across a
153 sequence of eight, five-year time intervals spanning the 40-year period of the study. We then use
154 time-specific species observations corresponding to these intervals as dependent variables in the
155 models that form the basis of our analyses, thereby enabling a fine-grain, temporally-explicit
156 view into historical patterns of changing climatic suitability.

157 Finally, we employ variable-specific ENM in our analysis: a tailored set of independent
158 variables is used for each of the five-year intervals in the time series. There is an increasing
159 awareness of the importance of variable selection in modeling environmental spaces [27,28,68–
160 72]. At the same time, the increased availability of large and sometimes novel environmental
161 data sets has made it difficult to select relevant predictors by anything other than automated or
162 semiautomated means [27,29,69,70,73]. The third way the work described here is distinctive is in
163 our use of NASA's MERRA/Max system to do automatic variable screening within each of the
164 temporally-aligned, five-year spans of our analysis.

165 MERRA/Max provides a scalable feature selection approach that enables direct use of
166 global climate model (GCM) outputs in ENM [74,75]. The system accomplishes this selection

167 through a MaxEnt-enabled Monte Carlo optimization that screens a collection of variables for
168 potential predictors of suitable conditions. Based on a machine learning approach to maximum
169 entropy modeling, MaxEnt is one of the most commonly-used software packages in the ENM
170 modeling community [76–78]. Among its many features, MaxEnt ranks the contribution of
171 predictor variables to the formation of its models. MERRA/Max's Monte Carlo method exploits
172 this capability in an ensemble strategy whereby many independent MaxEnt runs, each drawing
173 on a random pair of variables from within a large collection of variables, converge on a global
174 estimate of the top contributing variables in the collection being screened. Importantly, the
175 ensemble's bivariate MaxEnt runs can operate in parallel in a high-performance, cluster computer
176 environment, and, with a sufficient number of processors available, can do so in only a few
177 minutes, regardless of variable collection size.

178 With MERRA/Max, variable selection is guided by the indirect biological influences
179 injected into the algorithm's selection process by the species occurrence files, identifying
180 biologically and ecologically plausible predictors in large, multidimensional data sets where
181 selection through ecological reasoning or other means is not feasible [69,74,79]. In the current
182 study, the time-specific variable selection performed by MERRA/Max enables a view into the
183 changing patterns of environmental determinants of climatic suitability that would otherwise be
184 difficult, if not impossible, to obtain.

185 Collectively, these three aspects of the study offer a more detailed look at past patterns of
186 change in the climatic suitability for Cassin's Sparrow than have been previously reported. In the
187 sections that follow, we describe our method and results, discuss what we see as the important
188 take-away lessons, and conclude with recommendations for next steps.

189 Materials and Methods

190 We obtained the data used in this study from publicly available sources. We developed
191 scripts operating in the open-source R v4.1.3, Python 2.7.12, Java 1.8.0_261, and bash v5.0
192 environments to perform the computational work of the study. Input data and principal scripts
193 used in the study are available for download at: https://github.com/jschnase/MMX_Toolkit [80].

194 Occurrence data

195 To create a set of longitudinal occurrence records, we used the R rgbf library to obtain
196 Cassin's Sparrow observations from the Global Biodiversity Information Facility (GBIF) [81,82]
197 (GBIF.org; [15 January 2022] GBIF Occurrence Download <https://doi.org/10.15468/dl.x33grq>).
198 A total of 32,518, georeferenced records for the years 1980 through 2019 were downloaded.
199 More than 95% of the records were originally sourced from the eBird citizen-scientist
200 observational dataset [83], but the download also included research-grade records from
201 iNaturalist [84], the National Ecological Observational Network's (NEON) breeding land bird
202 point count collection [85], and museum specimen records from the National Museum of Natural
203 History (NMNH) [86], American Museum of Natural History (AMNH) [87], Harvard
204 University's Museum of Comparative Zoology [88], Kansas University [89], and the University
205 of Arizona [90].

206 We merged the observations into a time-series comprising eight, five-year aggregated
207 collections: 1980–84, 1985–89, 1990–94, 1995–99, 2000–2004, 2005–09, 2010–2014, and 2015–
208 19 (Fig 1A). These collections ranged in size from 263 records in the 1980 group to over 14,000
209 records in the 2015 collection. To reduce sampling bias, we applied two filtering steps. To avoid
210 the potential of double counting the same individual bird, we thinned the entire dataset to non-

211 overlapping observations within a 16 km (~10 mile) buffer based on the species' home range size
212 [2,5,17,21]. For count uniformity across the series and to reduce record-density influences that
213 can diminish model performance [91–94], we obtained random, 250-record samples for each
214 five-year span in the time series, which proved in subsequent tuning steps to be an optimal
215 sample size in the final models.

216 Environmental variables

217 We used data from the U.S. Geological Survey (USGS) National Gap Analysis Program
218 (GAP) to define a study area that encompasses the species' range across the continental U.S.
219 (latitude 24.8°N to 44.0°N and longitude 93.5°W to 115.6°W) [95]. We then created a *base*
220 *collection* of 30 M2 variables that we judged from personal experience and knowledge of the
221 literature to be potentially important environmental determinants of suitable conditions for
222 Cassin's Sparrow (Table 1, Fig 1A) [2,3,5,17,18]. These were drawn from four, hourly, time-
223 averaged, two-dimensional collections in which each variable represented one surface-level
224 spatial grid across the landscape: (1) M2T1NXSLV, consisting of air temperatures, wind
225 components, total precipitable water vapor, etc., at popularly-used vertical levels, (2)
226 M2T1NXFLX, consisting of surface fluxes, such as observation-corrected total precipitation,
227 surface air temperature, specific humidity, wind speed, and re-evaporation, (3) M2T1XRAD,
228 consisting of radiation estimates, such as surface albedo, cloud area fraction, cloud optical
229 thickness, solar radiation, and (4) M2T1NXLND, which is made up of an assortment of variables
230 of particular interest to environmental suitability modeling applications, such as surface soil
231 wetness, root zone soil wetness, soil temperatures at various layers, and important elements of
232 the land energy and water balance equations [34,96].

233 We obtained M2 data in its native, Network Common Data Form 4 (NetCDF4) format
234 from research collections housed in the NASA Center for Climate Simulation (NCCS) [97];
235 however, the data are also available to the general public through the Goddard Earth Sciences
236 Data and Information Services Center (GES DISC) [98,99]. We used the subsetting capabilities
237 of Python's xarray v2022.06.0 library [100] to assemble global, five-year aggregate collections
238 from the original downloads. These groupings corresponded to the eight intervals of our
239 occurrence data time series. Each five-year collection contained the averaged maximum,
240 minimum, and mean values for the 30 selected variables.

241 From this base collection, we assembled eight *working set* collections of averaged mean
242 values for the 30 variables, which we tailored to the specific requirements of the study using R's
243 rgdal v1.5-18 library [101]. Each environmental layer was clipped to the spatial extent of the
244 study area, which encompasses the geographic range of Cassin's Sparrow, re-projected, and
245 formatted for use by MaxEnt following the method of Hijmans et al. [102]. The resulting eight
246 working set collections corresponded to the eight intervals of our occurrence data time series. To
247 smooth the representation of local environmental conditions, we resampled the M2 layers from
248 their native spatial resolution of $1/2^{\circ}$ latitude \times $5/8^{\circ}$ longitude to 5.0 arc-minutes ($1/12^{\circ}$)
249 resolution (~7.6 km at latitude 35.0° N, which is within the study area) using the R raster v3.6-3
250 [103] library's bilinear interpolation routine.

251 In addition to the M2 collections, we built base and working set collections of M2-
252 derived bioclimatic variables, which we refer to as the MERRAclim-2 (MC) collections (Table
253 2). MC's variables are modeled on Worldclim's classic 19 bioclim variables, which were
254 designed to highlight climate conditions generally understood to relate to a species' physiology
255 [36,37]. The bioclim variables are derived from monthly maximum and minimum temperature

256 values and the average values for monthly precipitation. We built the M2 version of the bioclim
257 dataset using the R dismo v1.3-9 library's 'biowars' function [104] following the method used by
258 Vega et al. to generate the research community's first generation MERRAclim collection [105].
259 In their original formulation, Vega et al. [105] used the first-generation MERRA's two-meter
260 temperature (T2M) and two-meter specific humidity (QV2M) variables as inputs. In an
261 improvement over the earlier version of MERRA, the current, updated MERRA-2 provides a
262 modeled, observation-corrected total precipitation (PRECTOTCORR) variable expressed as a
263 mm/sec rate, which we adapted for use in MC by converting to a monthly amount [106].

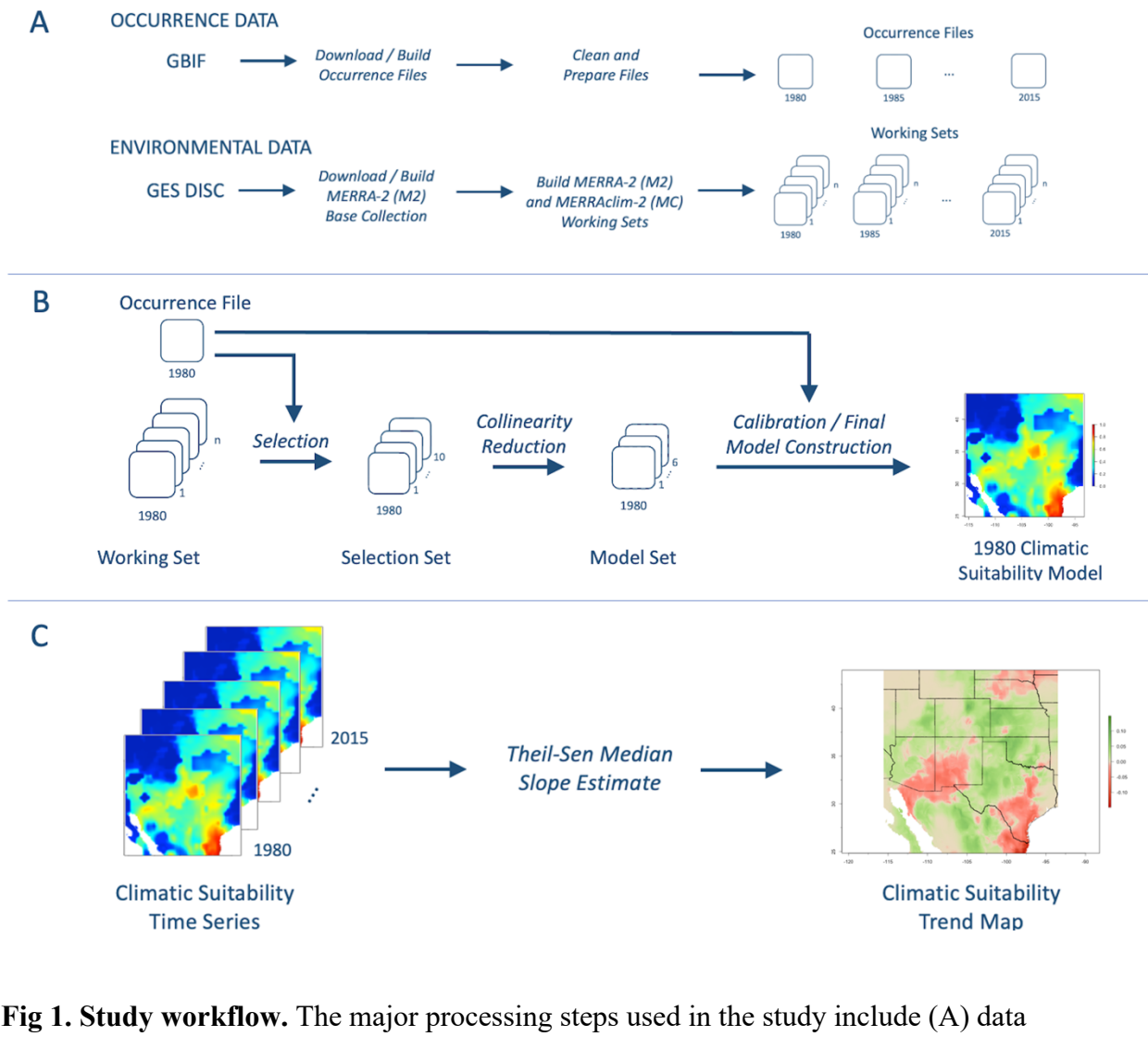


Table 1. MERRA-2 (M2) variables.*

M2T1NXSLV	2D Atmospheric single-level diagnostics collection
TS	Surface skin temperature (K)
QV2M	2-meter specific humidity (kg/kg)
T2M	2-meter air temperature (K)
M2T1NXFLX	2D Surface turbulent flux diagnostics collection
EFLUX	Positive latent heat flux (W/m ²)
HFLUX	Positive sensible heat flux (W/m ²)
SPEED	Surface wind speed (m/s)
PREVTOT	Total re-evaporation/sublimation of precipitation ((kg/m ²)/s)
PRECTOTCORR	Total observation-corrected surface precipitation ((kg/m ²)/s)
M2T1NXRAD	2D Surface and top-of-atmosphere radiation fluxes collection
ALBEDO	Surface albedo
LWGNT	Surface net downward longwave flux (W/m ²)
SWGNT	Surface net downward shortwave flux (W/m ²)
TAUTOT	Optical thickness of all clouds
CLDTOT	Total cloud area fraction
M2T1NXLND	2D Land surface diagnostics collection
LAI	Leaf area index
GRN	Vegetation greenness fraction (LAI-weighted)
GWETPROF	Average profile soil wetness
GWETROOT	Root zone soil wetness
TSURF	Mean land surface temperature (K)
TSAT	Surface temperature of saturated zone (K)
FRWLT	Fractional wilting area
QINFIL	Soil water infiltration rate ((km/m ²)/s)
GHLAND	Downward heat flux into topsoil layer (W/m ²)
WCHANGE	Total land water change per unit time ((kg/m ²)/s)
ECHANGE	Total land energy change per unit time (W/m ²)
PRMC	Total profile soil moisture content (m ³ /m ³)
RZMC	Root zone soil moisture content (m ³ /m ³)
EVPSOIL	Bare soil evaporation energy flux (W/m ²)
EVPTRNS	Transpiration energy flux (W/m ²)
EVPINTR	Interception loss energy flux (W/m ²)
EVLAND	Evaporation from land ((kg/m ²)/s)

271

* See Appendix A for a more detailed description of the M2 variables.

Table 2. MERRAclim-2 (MC) variables.

MC_Bio01	Annual mean temperature (°C)
MC_Bio02	Mean diurnal temperature range (°C)
MC_Bio03	Isothermality [(MC_Bio02/MC_Bio07)*100] (%)
MC_Bio04	Temperature seasonality [(Standard deviation*100)] (°C)
MC_Bio05	Maximum temperature of the warmest month (°C)
MC_Bio06	Minimum temperature of the coldest month (°C)
MC_Bio07	Temperature annual range (MC_Bio05-MC_Bio06) (°C)
MC_Bio08	Mean temperature of the wettest quarter (°C)
MC_Bio09	Mean temperature of the driest quarter (°C)
MC_Bio10	Mean temperature of the warmest quarter (°C)
MC_Bio11	Mean temperature of the coldest quarter (°C)
MC_Bio12	Annual precipitation (mm)
MC_Bio13	Precipitation of the wettest month (mm)
MC_Bio14	Precipitation of the driest month (mm)
MC_Bio15	Precipitation seasonality (Coefficient of variation) (%)
MC_Bio16	Precipitation of the wettest quarter (mm)
MC_Bio17	Precipitation of the driest quarter (mm)
MC_Bio18	Precipitation of the warmest quarter (mm)
MC_Bio19	Precipitation of the coldest quarter (mm)

272

273

274 Time series construction

275 Using the GBIF occurrence dataset, we constructed two time series spanning the years
276 1980 to 2019 in eight, five-year intervals. In the first, we used the M2 collections of working set
277 variables; in the second, we used the MC working sets. A two-step processing workflow was
278 applied to each five-year interval of each time series (Fig 1B). First, we used MERRA/Max to
279 screen the working set variables in each of the eight, five-year spans of the 40-year series. We
280 ran MERRA/Max on a dedicated testbed comprising a set of ten, 10-core Debian Linux 9 Stretch
281 virtual machines (VMs) in the NCCS's Explore high-performance cluster computing
282 environment [107]. Using MERRA/Max's standard screening configuration [74] and a per-
283 variable sampling rate of 100, we performed three screening runs, each returning a set of top ten
284 selected variables. We averaged the results of the three runs to create a *selection set* of the top
285 ten overall predictors for each five-year interval. We then used variance inflation factor (VIF)

286 analysis to reduce collinearities in the selected predictors. VIF shows the degree to which
287 standard errors are inflated due to the level of multicollinearities [108]. We calculated the VIF
288 for the selected variables using the R usdm v1.1-18 library and removed the least contributing
289 variable in any pair of variables having $r > 0.8$, $r^2 > 0.8$, and $VIF > 10.0$ [108,109]. This resulted
290 in a final, *model set* of top-recommended predictors for each five-year interval in the two time
291 series that had few if any multicollinearity issues.

292 Next, in a model calibration and final model construction step, we used the R ENMeval
293 v2.0.3 package [110,111] and MaxEnt v3.4.4 [112] to identify optimal feature class (FC) and
294 regularization multiplier (RM) settings for each set of occurrences and predictors in each of the
295 five-year intervals of the M2 and MC time series. MaxEnt's FCs are mathematical
296 transformations of the predictors that allow complex environmental dependencies to be modeled
297 and include linear (L), quadratic (Q), product (P), threshold (T), and hinge (H) settings; the RM
298 controls how closely-fitted the output distributions will be [76,113]. We tuned parameters by
299 performing a series of model runs across all possible combinations of six FCs (L, LQ, H, LQH,
300 LQHP, and QHP) and eight RM values ranging from 0.5 to 4.0 in increments of 0.5. The
301 combination of settings resulting in the lowest value for Akaike's information criterion corrected
302 for small sample size (AICc) [114] was taken to be an optimal tuning configuration, which was
303 subsequently used to construct a final model for each five-year interval in the two time series
304 [110,111]. For each of the 48 ENMeval calibration runs, and in the final MaxEnt model run, we
305 used 10,000 background locations randomly selected from across the study area and performed a
306 10-fold cross validation in which 70% of the occurrences were selected for training and 30% for
307 testing in each repetition [115,116]. Cloglog output scaling was used throughout. The cloglog
308 format gives an estimate between 0.0 and 1.0 of the probability of presence, which, in the current

309 study, we use as a proxy for environmental suitability [77]. The model calibration and final
310 model construction step was performed in triplicate for each five-year interval to produce an
311 averaged result that we used in the subsequent time series analysis.

312 Time series analysis

313 We adapted the approach of Stephens et al. [117] to assess the rate of change in Cassin's
314 Sparrow climatic suitability between 1980 and 2019. We used the Theil-Sen method to create
315 summary maps of the study area for each time series that showed regions of positive and
316 negative trend in suitability over the 40-year span of the study (Fig 1C). The Theil-Sen median
317 slope estimator provides a non-parametric means of robustly fitting a line to a set of points by
318 finding the median slope of all the lines through all pairs of points in the set. It is relatively
319 insensitive to outlying points and can be significantly more accurate than using simple, least
320 squares linear regression. In our case, the Theil-Sen median slope estimate was applied across
321 the eight raster layers comprising the final models of climatic suitability for each five-year
322 interval of our two 40-year time series. There were, thus, eight points in the slope calculation for
323 each cell in the resulting summary trend maps. We used the Mann-Kendall test to determine the
324 statistical significance of the resulting trends [118–120]. R's spatialEco v2.0-0 library was used
325 for the Theil-Sen and Mann-Kendall analyses [121].

326 We used the movement of weighted centroids to characterize the direction and speed of
327 shifts in climatic suitability. Weighted centroids represent the geometric center of all pixels in
328 the studied area weighted by their suitability index [122]. We chose centroids for this purpose
329 because of their ability to account for information derived across a species' entire modeled range
330 [123–125]. Our determination of the direction and speed of centroid movement was made by
331 measuring the vector between weighted centroids of the 1980 and 2015 probability maps using

332 R's enmSdmX library [126]. The direction of shifts was quantified in degrees ranging between
333 0° and 360°, with 0° being due north.

334 We complemented our look at biological responses with an analysis of trends in the
335 environmental variables underlying the time series models. First, we examined trends in the
336 values of the most contributory variables across the entire time series. Top contributing variables
337 were those that appeared in half or more of the 24 final models in the triplicated time series;
338 these variables were ranked by their permutation importance, which can range from zero (no
339 contribution) to one (high importance) [69,127]. For these study-wide top contributing variables,
340 we computed Theil-Sen slopes to assess trends and visualize patterns of change in the mean
341 values of each of M2's and MC's modeled variables over the past 40 years across the study area.
342 We then examined trends in the relative contributions of each of these top variables over time
343 (i.e., trends in each variable's permutation importance) on a per-interval basis across the 40-year
344 span of the study.

345 The final models produced in the calibration and final model construction step were
346 judged for reasonableness based on first-hand knowledge of the species and its climatic
347 preferences, what is known about Cassin's Sparrow's range from the published literature
348 [2,3,5,17], and observational records from Cornell Lab's eBird database [128]. To gain a
349 quantitative perspective on performance, we used the Area Under the Receiver Operating
350 Characteristic (ROC) Curve (AUC) as a measure of model accuracy. AUC is a measure of a
351 model's ability to discriminate presence from absence and ranges from 0.0 to 1.0 [129,130]. In
352 addition, we used the True Skill Statistic (TSS) [131,132] and Percent Correctly Classified
353 (PCC) [133] as measures of model accuracy, where higher values in both cases also indicate
354 greater accuracy.

355 Results

356 Model performance

357 In evaluating model performance, we regarded AUC measures < 0.7 as low, 0.7–0.9 as
358 moderate, and > 0.9 as high; similarly, we regarded TSS and PCC measures < 0.5 as poor,
359 0.5–0.8 as useful, and > 0.8 as good [134]. By these metrics, models exhibited moderate
360 performance across all 24 models per time series in their mean AUC, PCC, and TSS values
361 (Table 3). We judged this level of performance to be a reasonable basis for examining the broad
362 trend patterns displayed by the time series models, which were the primary focus of the study
363 [131–133]. Our distribution maps corresponded well with what is known about the natural
364 history of the species and maps derived from observational records [128].

365

Table 3. Model performance.*

Time Series	AUC	PCC	TSS
MERRA-2 (M2)	0.817 ± 0.009	0.718 ± 0.023	0.528 ± 0.017
MERRAclim-2 (MC)	0.812 ± 0.007	0.734 ± 0.008	0.789 ± 0.020

* Overall model performance for the M2 and MC time series. Mean ± standard error used throughout, n=24 in both time series.

366

367 Climatic suitability

368 The study area encompasses approximately $3.91 \times 10^6 \text{ km}^2$. Final models in the two time
369 series reveal changing patterns of estimated climatic suitability for Cassin's Sparrow across the
370 region over the past 40 years that reflect differences in the type of predictors used and,

371 presumably, actual changes in climatic suitability itself. On visual assessment, the most
372 favorable climatic conditions for the species have generally concentrated in the southeastern
373 regions of the study area according to both the M2 and MC time series; however, over time, a
374 northwesterly shift in areas of high suitability is apparent in both series (Figs 2A, 3A). The Theil-
375 Sen trend maps also show a northwesterly movement in increasing climatic suitability over the
376 past 40 years, although the patterns of change are more broadly diffuse in the M2 series, as
377 described in greater detail below (Figs 2B, 3B). An overall increase in climatic suitability was
378 identified over approximately 54.9% of the study area ($\sim 21.49 \times 10^5 \text{ km}^2$) in the M2 time series
379 and 69.5% of the study area ($\sim 27.21 \times 10^5 \text{ km}^2$) in the MC series (Table 4). Areas showing an
380 overall decrease in climatic suitability ranged in size from approximately 40.1% ($\sim 15.72 \times 10^5$
381 km^2) in the M2 time series to 24.4% of the study area ($\sim 9.54 \times 10^5 \text{ km}^2$) in the MC series.

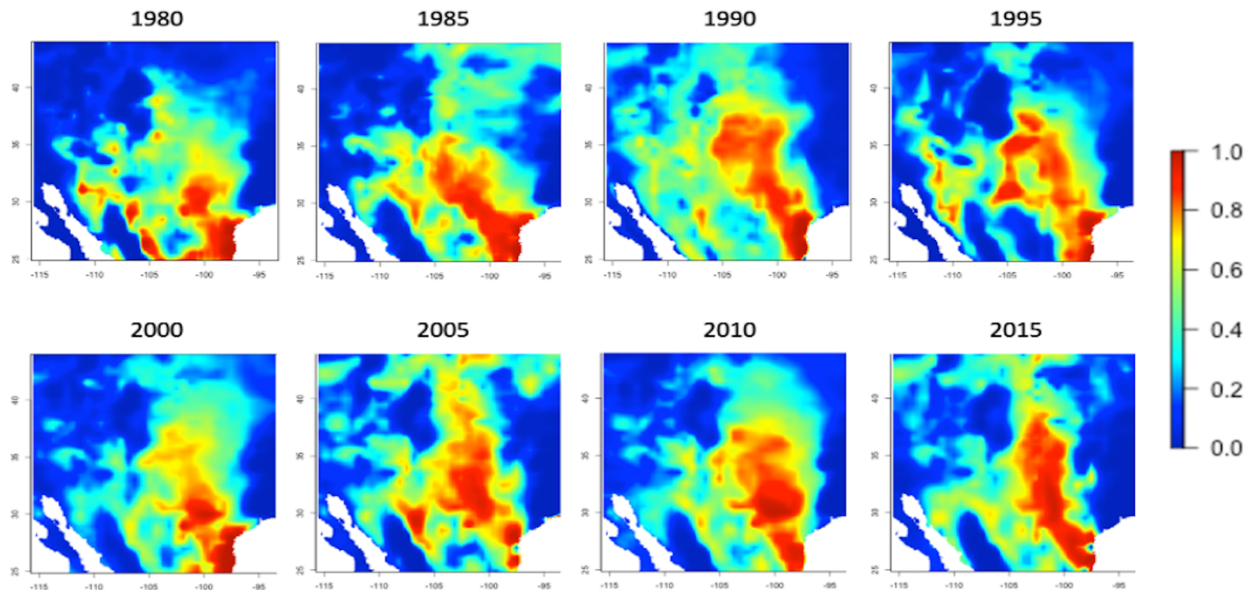
382 Focusing on areas of statistically-significant change provides a somewhat different
383 perspective. The absolute values of positive and negative change across the region are low, and
384 the areas where change can be identified as significant at the 95% confidence level are relatively
385 small (Table 4). While significant trends are hard to ascertain for time series in which $n=8$, for
386 the M2 series, the statistically-significant Theil-Sen results indicate that the estimated
387 probabilities of suitable climate have been increasing by an average of 0.03 every five years for
388 the past 40 years across 6.2% of the study area, with a corresponding average decrease in
389 estimated probabilities of 0.05 over 0.5% of the region. Significant positive trends were
390 concentrated in the central, northwestern, and far southwestern regions of the study area, while
391 negative trends concentrated in the southeast and central southwest, imparting a west to
392 northwesterly axis to these positive shifts that is consistent with the weighted centroid analysis,
393 as described below.

Table 4. Climatic suitability trends.*

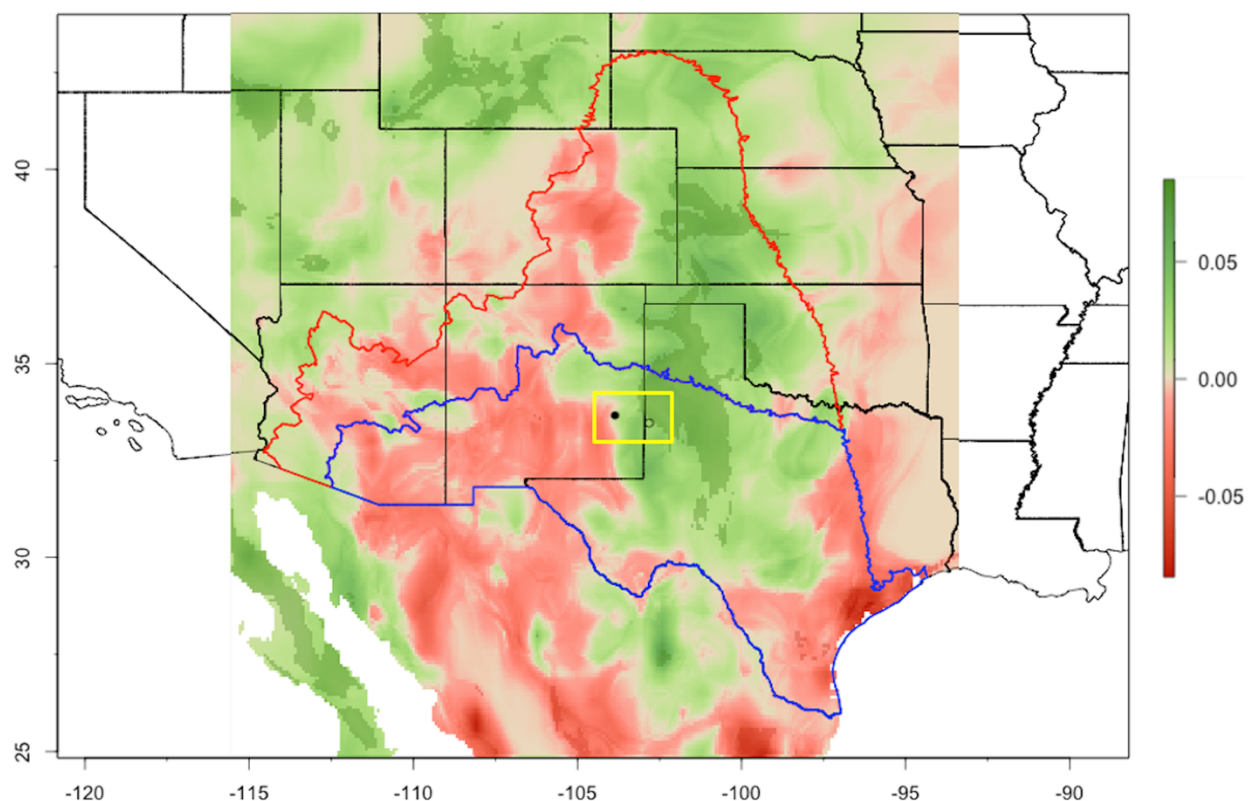
Time Series	Overall Trends		Significant Trends			
	km ² × 10 ⁵	% of area	Z	km ² × 10 ⁵	% of area	TS Δ / 5-yr
MERRA-2 (M2)	21.49 ± 3.96	54.9 ± 10.0	3.09 ± 0.01	2.41 ± 0.64	6.2 ± 1.6	0.03 ± 0.05
	15.72 ± 1.28	40.1 ± 3.2	-2.85 ± 0.15	0.19 ± 0.07	0.5 ± 0.2	-0.05 ± 0.01
MERRAclim-2 (MC)	27.21 ± 1.07	69.5 ± 2.6	3.34 ± 0.08	2.15 ± 0.11	5.5 ± 0.3	0.03 ± 0.01
	9.54 ± 0.06	24.4 ± 2.7	-2.09 ± 0.01	0.37 ± 0.05	0.9 ± 0.1	-0.06 ± 0.02

394 * Table presents a summary of results obtained from Theil-Sen median slope analysis of the study's two
395 time series. Trend areas are calculated for the map regions in Figs 2B and 3B that exhibited change at
396 any level of statistical significance (Overall Trends) as well as statistically-significant change at the 95%
397 confidence level (Significant Trends). Results are based on the three trend maps produced by the
398 triplicated runs in each time series and show mean ± standard error across these three maps. Positive
399 (green) and negative (red) trends are indicated by the corresponding positive and negative Mann-
400 Kendall Z scores. Theil-Sen slope values (TS) represent the rate of change in estimated probabilities of
401 climatic suitability per five-year interval across the 40-year time series in areas showing statistically-
402 significant trends.

MERRA-2 (M2) Climatic Suitability Time Series

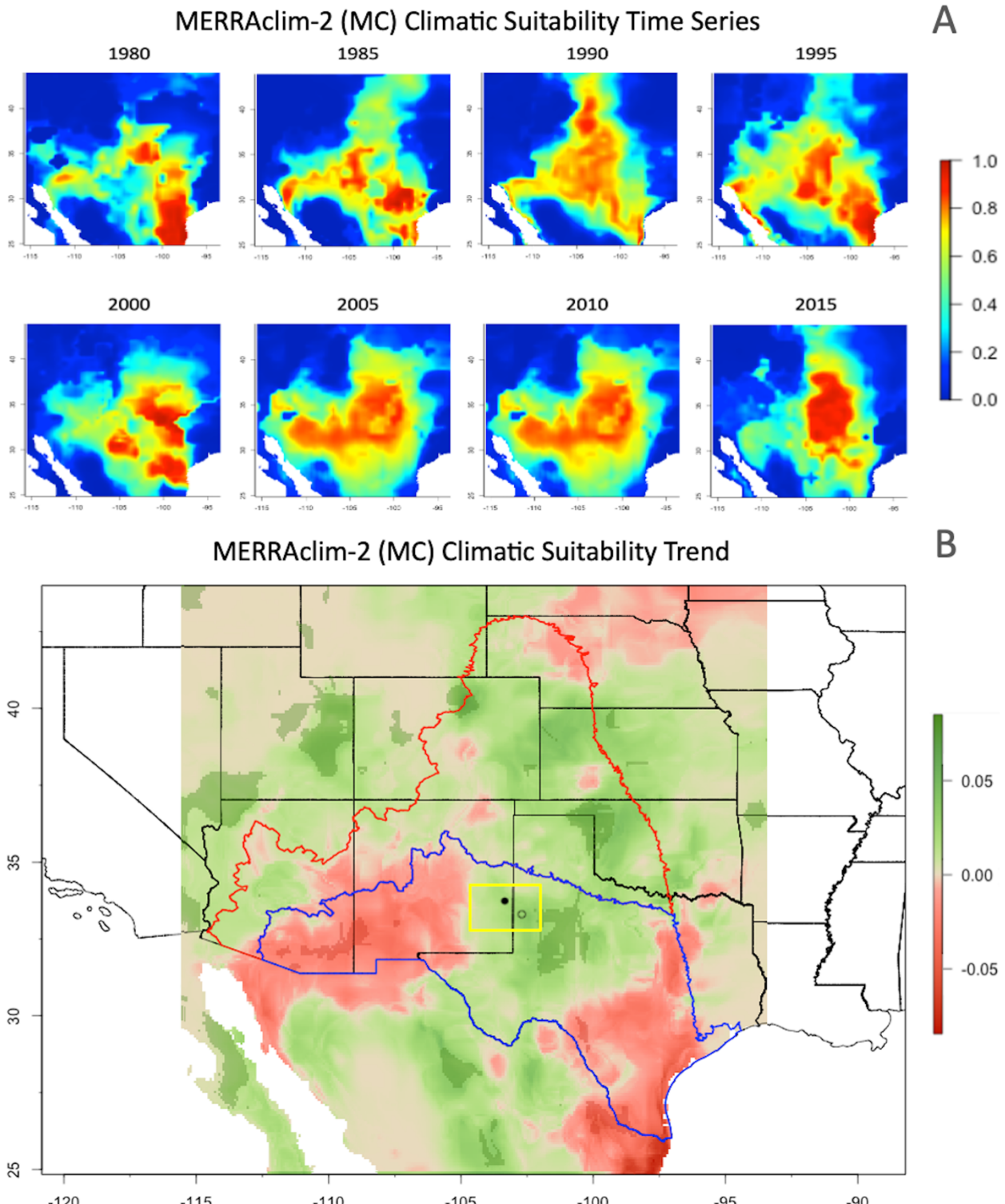


MERRA-2 (M2) Climatic Suitability Trend



403

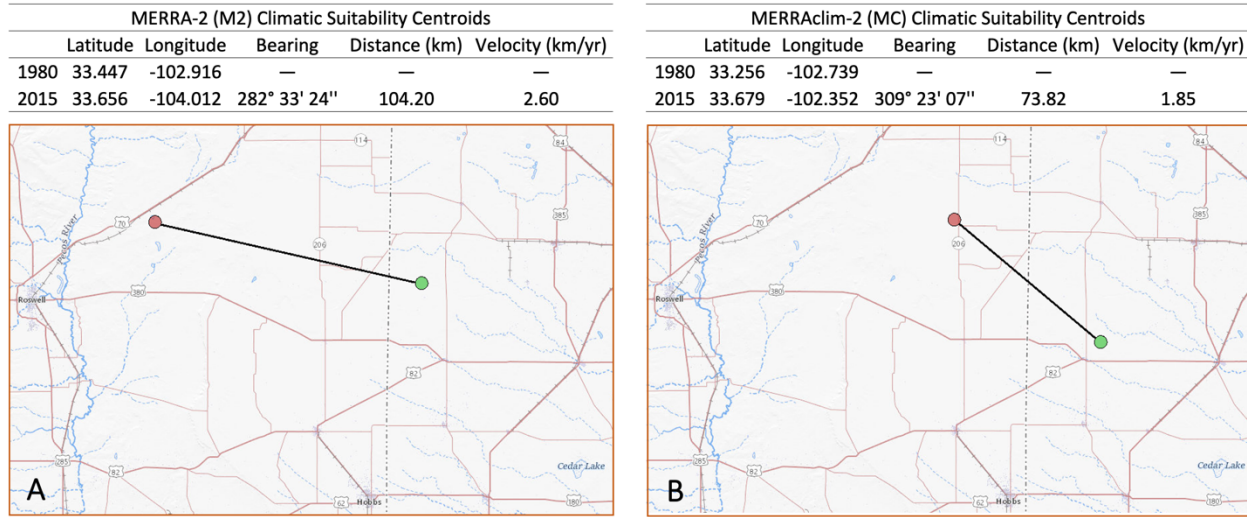
404 **Fig 2. MERRA-2 (M2) climatic suitability trends.** Averaged results from the three M2 time
405 series runs: (A) Estimated probabilities of climatic suitability for Cassin's Sparrow for the five-
406 year intervals spanning 1980 to 2019. Probability values range from 0.0 to 1.0 with warmer
407 colors indicating more favorable conditions. (B) Spatial distribution of Theil-Sen slopes showing
408 the rate of change in probabilities of climatic suitability per five-year interval across the 40-year
409 time series. Positive trends are indicated in green, negative trends in red. Statistically-significant
410 positive and negative trends at the 95% confidence level are shown in dark green and red,
411 respectively. Colored outlines indicate the northern extent of Cassin's Sparrow's U.S. breeding
412 (red) and non-breeding (blue) ranges. Cassin's Sparrow's summer, breeding range encompasses
413 all of the species' winter, non-breeding range. The yellow box shows the location of a shift in
414 weighted centroids for climatic suitability from 1980 (\circ) to 2015 (\bullet).



417 **Fig 3. MERRAclim-2 (MC) climatic suitability trends.** Averaged results from the three MC
418 time series runs. See Fig 2 caption for additional detail.

419 Theil-Sen results for the MC time series paint a similar picture. Statistically-significant
420 probability estimates of suitable climate have been increasing by an average of 0.03 every five
421 years for the past 40 years across 5.5% of the study area, with an accompanying average
422 decrease in estimated probabilities of 0.06 over 0.9% of the region (Table 4). Significant positive
423 trends concentrated in three clusters, one each in the northwest and northeast, the third in a
424 central southwestern region, which, by contrast, showed a negative trend in the M2 analysis.
425 However, there was a significant negative trend for the southeast region of the MC series that
426 coincides with the pattern observed for the M2 series.

427 Overall shifts in the climatic suitability for Cassin's Sparrow were observed in both time
428 series. The 40-year displacement of the weighted centroid for suitability in the M2 time series
429 was approximately 104 km and had a westerly inclination (282°). This pattern contrasted with
430 that seen in the MC time series, which showed a 40-year displacement of 75 km along a
431 northwesterly trajectory (309°) (Fig 4). Centroid movement in the M2 time series shows a higher
432 change velocity than that seen in the MC time series (2.60 km/yr vs. 1.85 km/yr respectively).



434 **Fig 4. Climatic suitability shifts.** Maps show direction, distance, and velocity of 40-year shifts
435 in the weighted centroids for climatic suitability in (A) the M2 time series and (B) the MC time
436 series from 1980 (●) to 2015 (●). For orientation, Roswell, NM is the city on the western
437 boundary of the maps. Base map courtesy of the USGS with annotations by the authors.

438

439 Environmental variables

440 The top contributing variables in the M2 time series were surface wind speed (SPEED),
441 bare soil evaporation energy flux (EVPSOIL), 2-meter specific humidity (QV2M), interception
442 loss energy flux (EVPINTR), optical thickness of all clouds (TAUTOT), total re-evaporation of
443 precipitation (PREVTOT), and surface net downward shortwave flux (SWGNT) (Table 5).
444 Theil-Sen analysis showed overall, positive trends across the study area for SPEED, QV2M,
445 PREVTOT, and SWGNT, with positive change centrally located in the study area for SWGNT,
446 concentrated in northern, northeastern, and southeastern regions in QV2M, and broadly scattered
447 in SPEED and PREVTOT (Fig 5). Predominantly negative trends were seen in EVPSOIL and
448 EVPINTR, with EVPSOIL's negative changes concentrated in the southwest and EVPINTR's

449 broadly distributed across the entire study area. Nearly equivalent areas of overall positive and
450 negative change were observed for TAUTOT, with positive change concentrated in the north and
451 southeast (Table 6). M2 trends generally lacked statistical significance.

452 The top contributing variables in the MC time series were mean temperature of the
453 wettest quarter (MC_Bio08), precipitation of the driest month (MC_Bio14), precipitation of the
454 warmest quarter (MC_Bio18), isothermality (MC_Bio03), precipitation seasonality (MC_Bio15),
455 maximum temperature of the warmest month (MC_Bio05), and precipitation of the wettest
456 month (MC_Bio13) (Table 5). The Theil-Sen studies showed predominantly positive trends
457 across the study area for MC_Bio08, MC_Bio15, and MC_Bio05, with large expanses of
458 positive change concentrated centrally and in the northwest region of the study area for
459 MC_Bio05, concentrated in the southwest for MC_Bio08, the west and southwest for MC_Bio15
460 (Fig 5). Negative trends dominated in MC_Bio14 and MC_Bio18, with westerly-inclined,
461 broadly diffuse patterns of change generally concentrated in the west for both variables. Nearly
462 equivalent areas of positive and negative change were seen in MC_Bio03 and MC_Bio13, with
463 broadly scattered patches of change apparent for each variable throughout the study area (Table
464 6). Most of the trends observed in the MC variables also lacked statistical significance.

465 Finally, time-specific variable selection also enabled a view into each variable's
466 contributory trend across the 40-year span of the time series (Fig 6). In the M2 time series, we
467 observed a generally increasing trend in the relative contribution of EVPINTR to each five-year
468 interval's final model and a generally decreasing trend in the contributions of QV2M and
469 SWGNT. SPEED and EVPSOIL were consistently high contributors across the board; TAUTOT
470 and PREVTOT were consistently moderate contributors. In the MC time series, MC_Bio14 and
471 MC_Bio03 show generally increasing trends; MC_Bio08 showed sharply decreasing trends.

472 MC_Bio18 was a consistently high contributor across the series, with MC_Bio15, MC_Bio05,

473 and MC_Bio13 making consistent contributions at moderate to low levels.

474

Table 5. Top contributing variables.*

MERRA-2 (M2)	n	PI	Description
SPEED	24	18.3 ± 1.7	Surface wind speed (m/s)
EVPSOIL	24	12.4 ± 1.9	Bare soil evaporation energy flux (W/m ²)
QV2M	24	6.2 ± 1.2	2-meter specific humidity (kg/kg)
EVPINTR	20	19.3 ± 1.5	Interception loss energy flux (W/m ²)
TAUTOT	17	9.9 ± 1.8	Optical thickness of all clouds
PREVTOT	15	16.4 ± 2.9	Total re-evaporation/sublimation of precipitation ((kg/m ²)/s)
SWGNT	13	20.8 ± 2.8	Surface net downward shortwave flux (W/m ²)

MERRAclim-2 (MC)	n	PI	Description
MC_Bio08	24	39.6 ± 3.1	Mean temperature of the wettest quarter (°C)
MC_Bio14	19	11.1 ± 1.0	Precipitation of the driest month (mm)
MC_Bio18	18	23.2 ± 2.9	Precipitation of the warmest quarter (mm)
MC_Bio03	16	10.7 ± 2.0	Isothermality [(MC_Bio2/MC_Bio07)*100] (%)
MC_Bio15	15	10.6 ± 1.3	Precipitation seasonality (Coefficient of variation) (%)
MC_Bio05	15	9.2 ± 3.7	Maximum temperature of the warmest month (°C)
MC_Bio13	12	8.1 ± 2.6	Precipitation of the wettest month (mm)

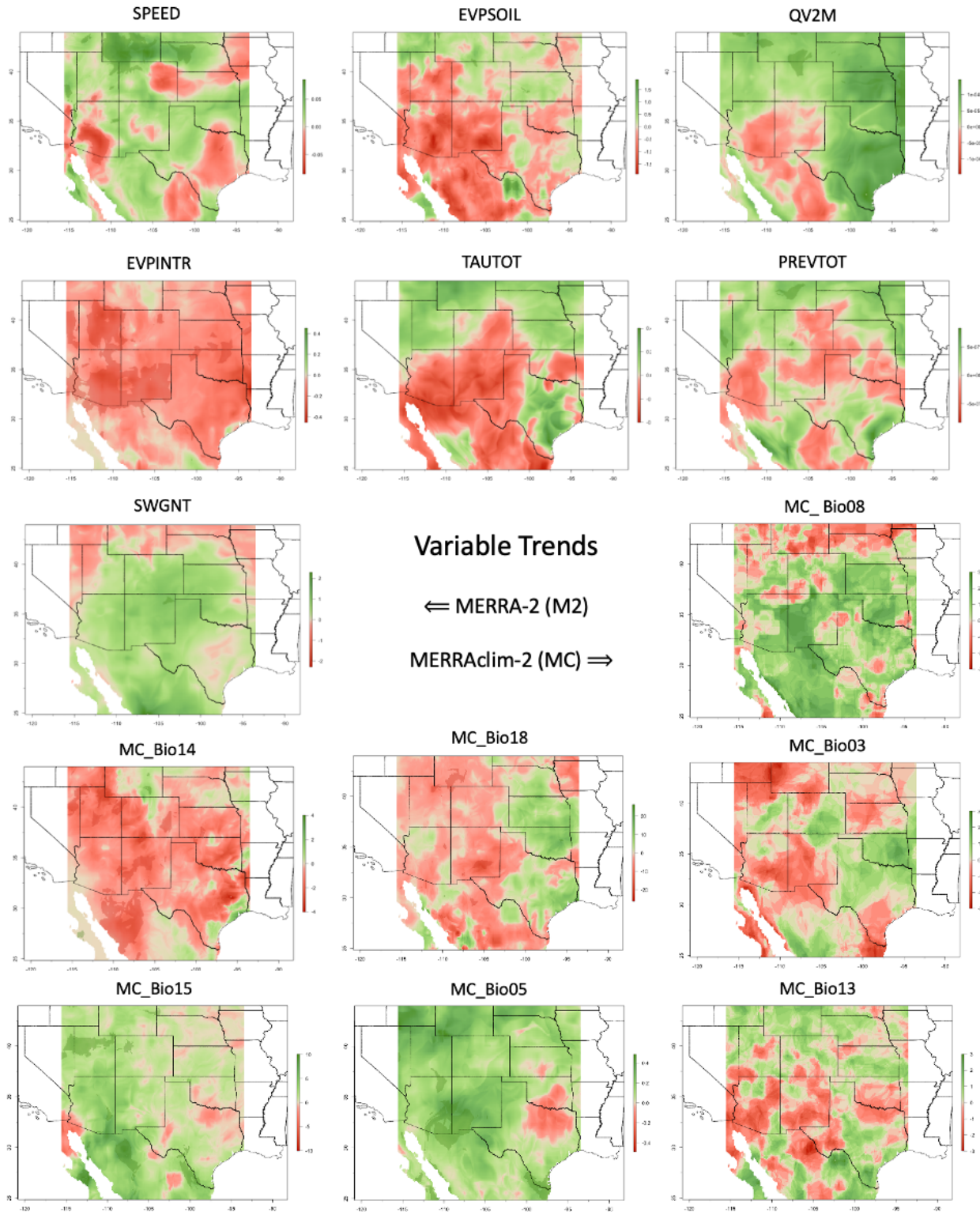
475

476 * Table presents a summary of the top contributing variables in the study's M2 (top) and MC (bottom)

477 time series. Variables are ordered first by the number of times the variable appeared in the final

478 models of the eight, five-year intervals of the triplicated times series (n), followed by the variable's

479 mean permutation importance (PI) ± standard error across those appearances.

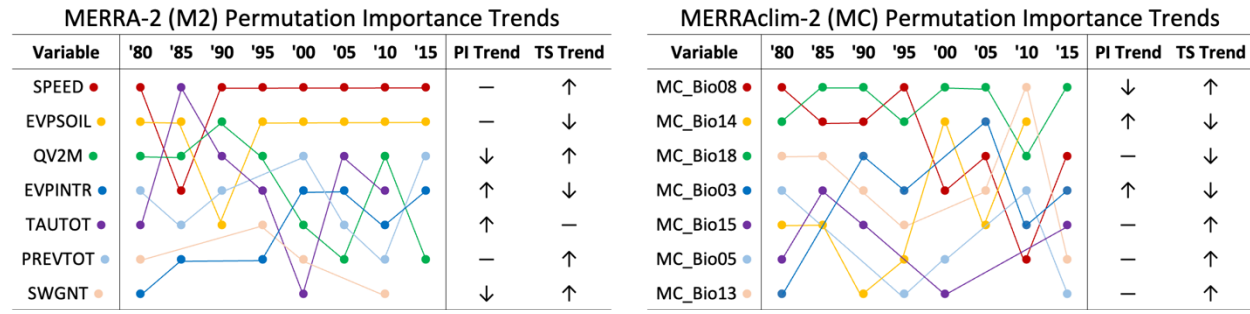


481 **Fig 5. Variable trends.** Maps show the Theil-Sen slope estimates for the top contributing
482 variables in the M2 and MC time series (Table 5). Positive trends are shown in green; negative
483 trends are shown in red. Color intensity represents the rate of change in the units of measure for
484 the variable per five-year interval across the 40-year time series. Maps created by the authors.

Table 6. Variable area trends *

Variable	% of area	Variable	% of area
SPEED	62.5 -29.8	MC_Bio08	67.5 25.5
EVPSOIL	34.4 -63.1	MC_Bio14	17.2 73.3
QV2m	75.0 -22.3	MC_Bio18	36.5 62.1
EVPINTR	5.0 76.7	MC_Bio03	44.4 53.4
TAUTOT	46.1 53.4	MC_Bio15	80.0 14.8
PREVTOT	57.5 41.7	MC_Bio05	85.6 7.9
SWGNT	79.5 20.4	MC_Bio13	54.6 43.7

485 * Table shows results from the Theil-Sen analysis of the top
486 contributing variables in the study's M2 and MC time series. Positive
487 (green) and negative (red) trend coverage areas represent the trend
488 proportion across the entire study area and are calculated for the
489 map regions in Fig 5 that exhibited overall change at any level of
490 statistical significance.



491
492

493 **Fig 6. Permutation importance trends.** Diagrams showing the relative contributions of the top
494 contributing variables across the five-year intervals of the M2 (left) and MC (right) time series
495 over the 40-year span of the study. The PI Trend column indicates whether a variable's relative
496 contribution to a five-year interval's final model is generally increasing (↑), decreasing (↓), or
497 remaining constant (—) across the 40-year span of the series. For comparison, the TS Trend
498 column shows each variable's overall net positive or negative Theil-Sen trend coverage area from
499 Tables 6. Variables are listed in descending order of overall contribution to the time series, as
500 shown in Table 5.

501 **Discussion**

502 **Climatic suitability**

503 The most important finding in the current study is that climatic suitability for Cassin's
504 Sparrow has been changing over the past 40 years, and those changes are manifest across the
505 landscape as a complex pattern of positive and negative trends that can yield varying and
506 sometimes contradictory interpretations depending on how suitability is modeled and the context
507 in which modeled results are viewed. From a study-wide perspective, the northwesterly shift in
508 favorable conditions we observed across both time series is consistent with what has been
509 reported for Cassin's Sparrow and many North American grassland bird species [8,135–137]. In
510 addition, our velocity results are on par with other estimates. Bateman et al. [8], for example,
511 found an average bioclimatic velocity of 1.27 km/yr to the west, northwest, and north over the
512 past 60 years in the potential breeding distributions of 285 species of land birds across the
513 continental U.S., with some potential breeding populations shifting at rates up to 5.51 km/yr.
514 Likewise, a recent study by Huang et al. [124] reported a mean bioclimatic velocity of 2.25
515 km/yr in 29 species of grassland birds along predominantly east-west axes of increasing
516 environmental suitability, accompanied by an estimated, mean abundance-based velocity of 5.02
517 km/yr along more northerly inclined axes of increasing abundance. This leads us to believe we
518 are seeing meaningful patterns with the approach we have taken. Assuming that is the case, these
519 broad results belie potentially important details revealed by a more granular view.

520 For example, the MC time series paints a more favorable picture of changing conditions
521 than what is seen in the M2 time series: climatic conditions are generally improving in the
522 former, in the latter we see an overall decline. This contrast is particularly apparent across the

523 western regions of the study area and within the USGS GAP boundaries of Cassin's Sparrow's
524 northernmost breeding range. In the west, M2-driven model results portray a northerly shift in
525 improving conditions across the full extent of the study area. With the MC-driven models,
526 changes are not nearly as distinct nor are they as extensive. M2-driven model results show
527 sharply improving climatic suitability in the northeastern extent of the breeding range and a fall-
528 off along the western boundaries of its breeding and non-breeding ranges, while the MC-driven
529 model results show improving climatic suitability in the northeastern region and a fall-off along
530 only the western boundary of Cassin's Sparrow's breeding range.

531 The differences between the two time series become even more noticeable when the
532 scope is reduced to the state level. Seven states comprise Cassin's Sparrow's breeding and non-
533 breeding ranges within the continental U.S.: Arizona (AZ), Colorado (CO), Kansas (KS),
534 Nebraska (NE), New Mexico (NM), Oklahoma (OK) and Texas (TX) (Figs 2B, 3B; Table 7).
535 According to the GAP range maps, Cassin's Sparrow is found in four of these states only during
536 the breeding season (i.e., CO, KS, NE, and OK). With KS and OK, we see similar trend patterns
537 across the two time series. On the other hand, for CO, we see a sharp decline in suitability in the
538 M2 time series, especially in the central part of the state, and a general improvement in
539 conditions in the MC time series. We see the inverse pattern for NE across the two time series.

540 Within the U.S., Cassin's Sparrow has historically been most abundant in AZ, NM, and
541 TX [2,3,5,138,139]. These states represent the heart of Cassin's Sparrow's U.S. range, and it is
542 here we see the species move from non-breeding to breeding areas between winter and summer
543 months. This is also where we see the most striking differences in the M2 and MC time series'
544 model results. In the M2 series, climatic suitability in areas that historically accommodated
545 seasonal range expansion, between the non-breeding and breeding seasons, is shown to have

546 been declining over the past 40 years in AZ and NM. In contrast, climatic suitability in these
547 areas appears to be improving or largely unchanged in the MC series. In TX, M2 model results
548 indicate improving breeding season conditions in northern regions and decreasing suitability
549 along the state's southern border in breeding and non-breeding areas; similar but less pronounced
550 patterns are observed in the MC time series.

551 Taken together, these findings are consistent with recent work showing that the nature,
552 direction, and magnitude of changes in a species' climatic niche are not uniform, but rather
553 multidimensional in nature and shaped by complex, species-specific interactions that are
554 sensitive to environmental drivers other than temperature and precipitation alone
555 [122,124,140,141]. The findings also draw us into a consideration of the complexities that exist
556 in the relationship between population abundance and environmental suitability that may speak
557 to the ambiguities we see surrounding Cassin's Sparrow's conservation status.

558 Demographic attributes, such as abundance, are a crucial component of essentially all
559 species conservation decision-making processes. For example, population size is a factor in
560 NatureServe's conservation status evaluations [142], which, together with the USGS's North
561 American Breeding Bird Survey (BBS) population trend estimates [143], contribute in some way
562 to nearly all U.S. SWAPs and the identification of Species of Greatest Conservation Need
563 (SGCN) [144]. Given that data on species occurrences are far more common and readily
564 accessible than data on species abundance, it is not surprising that a significant amount of
565 research has focused on clarifying the abundance-suitability (AS) relationship and the extent to
566 which ENM-derived estimates of environmental suitability can serve as a proxy for population
567 abundance [145]. While much remains to be learned about modeling the distribution of
568 abundance, a consensus appears to be emerging around the following points:

569 (1) the distribution of environmental suitability based on bioclimatic variables
570 alone generally shows little, if any, correlation with the distribution of
571 abundance [124,146–148];

572 (2) the combination of bioclimatic predictors with other environmental attributes,
573 such as EFAs, edaphic variables, topographic data, vegetation indices, etc.,
574 can capture the influence of factors affecting abundance rather than just
575 occurrence, thereby yielding suitability model results that are often highly
576 correlated with abundance [145,147–149], and, in some cases, reflect well the
577 mean and maximal local abundances of a species [150];

578 (3) the AS correlation is particularly strengthened when the added non-climatic
579 predictors capture, in one way or another, environmental drivers that influence
580 fitness, dispersal, recruitment, or other demographic properties of a species
581 [149,151–153]; and

582 (4) correlative ENM that takes into account this bioclimatic-demographic
583 connection can provide practical benefits to spatial conservation efforts, such
584 as readily-attainable, large-scale abundance estimates; hot-spot identification;
585 and reduced survey and monitoring costs [24,145,147,148,150].

586 Our findings are consistent with the first point: we see different patterns of historical
587 change in environmental suitability depending on whether time series models are driven by
588 bioclimatic variables alone or by variables more aligned with ecological functioning, and
589 therefore potentially species demography. We also see that state-level, climatic suitability trends
590 in both time series appear to have little in common with three major, state-level, abundance-

591 driven conservation status assessments in force today (Table 7). Finally, the differences we
592 observe among the suitability distributions of both time series' five-year interval maps (Figs 2A,
593 3A), point to varying and potentially important underlying temporal dynamics. This leads us to
594 believe that modeled estimates of Cassin's Sparrow's distribution based on climatic suitability
595 can vary widely depending on the temporal frame in which they are constructed, the spatial
596 extent considered, and the environmental drivers being used. Furthermore, this variability can
597 lead to differing conclusions regarding the conservation status of the species, which likely mirror
598 the ambiguities we see in the current literature regarding the status of Cassin's Sparrow. We
599 cannot address the remaining points relating to the AS relationship at the moment, because we
600 did not combine M2 and MC variables in the current study, nor did we directly compare our
601 suitability results with demographic results. However, as described below, points (2) through (4)
602 do help us frame what we believe are important next steps in this line of research.

Table 7. Comparison of state-level trends.

M2		MC		BBS	NatureServe	SWAP
Br	NBr	Br	NBr	Br	—	—
AZ	↓	↓	↑↓	↓	↑	As
CO	↓	—	↑	—	↑	As
KS	↑	—	↑	—	↓	Vu
NE	↑	—	↑↓	—	↑	Vu
NM	↓	↓	↑↓	↓	↑	As
OK	↑	—	↑	—	↑	Im
TX	↑	↑↓	↑	↑↓	↓	Se

603 * Summary of the dominant, state-level climatic suitability trends during the
604 breeding (Br) and non-breeding (NBr) seasons from the M2 and MC time series.
605 The summary is derived from the Br and NBr range extents shown in the Thiel-
606 Sen maps of Figs 2B and 3B. Green arrows (\uparrow) indicate an overall larger area of
607 increasing climatic suitability trend, red (\downarrow) an overall larger area of decreasing
608 trend. A generally balanced overall trend is indicated by the presence of yellow
609 arrows ($\uparrow\downarrow$). Breeding Bird Survey (BBS) arrows reflect increasing and
610 decreasing state-level population trends from 1980 through the 2021 survey
611 year. The NatureServe and State Wildlife Action Plan (SWAP) assessments are
612 derived in slightly different ways but reflect the current, overall state-level
613 status as reported for each respective state. Abbreviations reflect the
614 terminology used in the different, state-level assessments: apparently secure
615 (As), vulnerable (Vu), imperiled (Im), stable (St), secure (Se), susceptible to
616 rapid population change (Su), and population trend unknown (Un).

617 Environmental variables

618 It is not surprising that the two collections of independent variables used to drive our two
619 time series of models should result in different patterns of historical climatic suitability change.
620 Studies have consistently demonstrated that correlative suitability models based on bioclimatic
621 variables alone capture different environmental dynamics compared to models based on
622 attributes of potentially more direct biological significance to a species [27,49,154]. Further,
623 while temperature and precipitation are far and away the most frequently used predictors in ENM
624 studies, and often end up being the most important [155], it has been shown that conditions
625 beyond these two variables exert a strong influence on bird distributions [8,156]. It is also not
626 surprising that the MC-based time series shows more favorable historical trends overall than
627 what we observed in the M2 time series. Studies have shown that the use of bioclimatic
628 predictors alone tends to overestimate range size, presumably because of their inability to
629 effectively account for all of a species' use of space and all the microclimatic influences to which
630 the species may be responding [157]. What we do find interesting is what appears to be the
631 enhanced capacity to discriminate between different forcings on a species over time that results
632 from combining time-specific variable selection with time-specific ENM.

633 In earlier work, we found evidence that MERRA/Max's Monte Carlo approach to
634 automated variable selection was capable of surfacing ecologically-plausible predictors from
635 multivariate collections [74,75,158–160]. Given the developmental nature of the approach, that
636 work focused on applying the technique to a single temporal frame of reference. Here, variable
637 selection has been applied to specific time intervals across a 40-year time series. This gives us an
638 opportunity to consider two types of trends in the selected environmental predictors: we can

639 examine how the most influential determinants of climatic suitability change over time and the
640 extent to which the relative contributions of those variables change over time.

641 Take, for example, the three most important variables in the MC time series: mean
642 temperature of the wettest quarter (MC_Bio08), which appears to have been generally increasing
643 across Cassin's Sparrow's range over the past 40 years while declining in importance as an
644 environmental driver; total precipitation of the driest month (MC_Bio14), which has been
645 decreasing across Cassin's Sparrow's range while increasing in importance as an environmental
646 driver over the same period of time; and precipitation of the warmest quarter (MC_Bio18),
647 which has also been generally decreasing across the species' range, but across a discontinuous
648 patchwork of positive and negative trends while remaining one of the top environmental drivers
649 over the 40-year span of the study (Table 6, Fig 6). Collectively, these three variables appear to
650 confirm that the long-running drought conditions across southwestern North America have had a
651 major influence on climatic suitability for Cassin's Sparrows [161,162]. That MC_Bio18 is
652 consistently the most important contributing variable across the time series is particularly
653 notable. A case can be made that MC_Bio18 essentially characterizes the seasonal precipitation
654 trends of the North American Monsoon, which has a recognized influence on the life history and
655 breeding biology of the species.

656 The North American Monsoon is a product of seasonal change in the atmospheric
657 circulation patterns that occurs as the summer sun heats the continental land mass. During much
658 of the year, the prevailing wind over northwestern Mexico, Arizona, and New Mexico is
659 westerly and dry. As the summer heat builds over North America, a region of high pressure
660 forms over the Southwest, and the wind becomes more southerly, drawing moisture from the
661 Pacific Ocean, Gulf of California, and Gulf of Mexico. In the Continental U.S., this circulation

662 brings thunderstorms and rainfall to Arizona, New Mexico, Southern California, Utah, and
663 Colorado, providing much of the region's annual total precipitation [163–167]. Importantly, apart
664 from the spatial variability that is directly related to topography, there is much intraseasonal and
665 interannual variability in the intensity and extent of monsoon rainfall, particularly in the
666 southwestern U.S. and northwestern Mexico [168], which may explain the broken and overall
667 weaker trend patterns observed in our results for MC_Bio18 (Fig 6).

668 Cassin's Sparrow's responsiveness to rainfall and apparent ability to quickly relocate
669 throughout the summer months in order to track optimal conditions for breeding has been a
670 repeating theme in the literature for nearly a century: it is a life history trait that has been the
671 source of much uncertainty about the species' range and abundance [2,3,5,18,20,139]. The model
672 contribution trends of the three top predictors in the MC time series, when set alongside
673 landscape-scale trends in the variables themselves, appear to point to the importance of monsoon
674 precipitation over Cassin's Sparrow's southwestern North American range over the past 40 years
675 as temperatures and overall drying conditions have increased across the region [161,162]. The
676 next two most contributory variables are isothermality (MC_Bio03) and precipitation seasonality
677 (MC_Bio15). Isothermality represents temperature evenness by quantifying how large the day-
678 to-night temperature oscillation is compared to the summer-to-winter oscillation. Our results
679 show a generally decreasing trend across the landscape (i.e., greater levels of annual temperature
680 variability relative to an average day) over the past 40 years, while the variable's importance as a
681 driver increases. Precipitation seasonality is a measure of the variation in monthly precipitation
682 totals over the course of the year. Our results show an increasing trend in precipitation
683 seasonality as the variable itself remains a consistent model contributor. Taken together, the
684 increasing and continuing importance of these two variables suggests that variability in both

685 temperature levels and precipitation amounts has had a major historical influence on climatic
686 suitability for Cassin's Sparrow as well. The remaining, contributing variables both have a nexus
687 with the monsoon season and drying conditions. In particular, precipitation of the wettest month
688 (MC_Bio13) generally occurs during the monsoon season and the maximum temperature of the
689 warmest month (MC-Bio05) generally precedes the onset of the monsoon season. Both of these
690 variables show an increasing trend over the past 40 years, and both are consistent, low-level
691 drivers in our results.

692 This interpretation of the importance of drying trends also appears to be supported by the
693 patterns we see in the M2 time series, just at a different scale. In particular, the top contributing
694 variables in the MC time series provide insights into the way macroclimatic change has
695 potentially influenced seasonal trends while the most important variables in the M2 time series
696 address various microclimatic and ecological functioning aspects of surface energy and
697 hydrological dynamics (Table 6, Fig 6) [34,35,169,170]. The two most important variables in the
698 M2 time series are surface wind speeds (SPEED), which appears to have been generally
699 increasing across the south southwestern region of the study area over the past 40 years while
700 remaining a consistently top model contributor, and bare soil evaporation energy flux
701 (EVPSOIL), which is generally decreasing across the same area over this period while also
702 remaining a top contributor across the time series. Wind has a mixing effect on the air near the
703 ground surface that can increase the evaporation of water from soil and plant surfaces until a
704 point is reached where drying conditions take over, as it appears to have occurred for the soil but
705 not yet for plants. Water loss from plant surfaces, reflected as interception loss energy flux
706 (EVPINTR), the fourth most contributory variable, has been increasing over the past 40 years
707 while its importance as a driver in our models has steadily increased. A similar pattern is seen in

708 the sixth most contributory variable, total re-evaporation of precipitation (PREVTOT), which is a
709 measure of precipitation efficiency (i.e., the amount of falling precipitation that evaporates or
710 sublimates before reaching the ground). In our results, there has been an overall increasing trend
711 in PREVTOT across the study area while the driver itself has remained a moderately consistent
712 in importance across the 40-year span of the study. These variables, along with increasing
713 shortwave radiant energy from the sun (SWGNT), modulated by variably decreasing clouds
714 across the North American Southwest (TAUTOT), contribute to observed conditions of absolute
715 humidity (QV2M), which, on balance, at this point, have been generally increasing across the
716 study area while decreasing in importance as an environmental driver [171–173]. Taken together,
717 the top contributing variables in the M2 time series suggest that microclimatic drying, with more
718 evaporation and less rainfall reaching the ground, may be the particular aspects of the varying
719 monsoon precipitation pattern of importance to Cassin's Sparrow.

720 This observed connection between top contributing variables, monsoon rainfall, and
721 ground-level drying conditions is consistent with what is known about Cassin's Sparrow's
722 ground-dwelling habit and the importance of microclimatic conditions to almost all aspects of
723 the species' life. Our results are also consistent with research showing that increasing
724 temperatures, increased temperature and precipitation variability, and drying soils are potent
725 drivers of environmental suitability at scales germane to many species found across the arid
726 grasslands of the southwestern U.S. [174,175]. However, given the importance of Cassin's
727 Sparrow's areal flight song behavior to the species' breeding ecology, the increase in surface
728 wind speed may have the most pronounced impact on climatic suitability and the species'
729 demography overall: male Cassin's Sparrows simply do not skylark when it is windy [17].

730 What then are the take-away lessons from our analysis of environmental variables? For
731 one, as noted by others, the juxtaposition of trend perspectives across two collections of
732 predictors seems to provide a more holistic view of climate-species interactions than might be
733 obtained from either collection on its own [49,55]. What is more, the automated, observation-
734 guided, time-specific selection of variables appears to provide an integrated view across the two
735 time series: the two collections of predictors seem to tell different parts of the same story about
736 what might be driving change.

737 That being said, these results must be interpreted with caution. M2 variables represent
738 the low-level physical drivers of many of the Earth system's biological processes [27,176]: an
739 interpretation of ecological plausibility could be made for many of the M2 variables. Studies
740 have shown, however, that MaxEnt's ranking of variable importance can capture biologically
741 realistic assessments of factors governing range boundaries when models are built using best-
742 practice procedures and variables are ranked based on permutation importance [69,79]. With
743 Cassin's Sparrow, we have a species whose behavioral and energetic ecology has been studied in
744 detail, facilitating the interpretation of relationships with M2 variables [17]. Of the many
745 potential contributors in the M2 and MC collections, the top contributing variables identified in
746 the two time series are known to be important environmental influences for the species and are
747 consistent with our mechanistic, process-based understanding of the bird's natural history
748 [2,17,177–179]. At this point, we feel confident saying that, in future modeling efforts,
749 spatiotemporal attributes of North American Monsoon precipitation, hydrologic conditions of the
750 soil, and surface winds should be considered variables of particular ecological relevance to
751 Cassin's Sparrow and key to understanding the species' conservation status.

752 **Conclusions**

753 This is a preliminary study, much of it qualitative, and all of it based on an experimental
754 modeling protocol and suite of technologies that are still very much in development. While we
755 see useful outcomes in what we have described here, our single biggest caution is that more work
756 needs to be done to elevate overall confidence in the approach. We need experience applying
757 retrospective ENM to different species, species assemblages, and different taxonomic groups.
758 We also we need experience using larger and more diverse predictor collections as the source
759 pool for variable screening, such as including a full range of topographic and edaphic data,
760 vegetation indices, remotely sensed EFAs, and data on land-cover/land-use change.

761 Throughout this effort, we have tried to strike a balance between precision and
762 scalability. It is likely that greater model accuracy across our time series could be attained by
763 carefully considered variable selection and manual tuning. However, our workflow can be fully
764 automated: the study presents a scalable approach to evaluating historical climatic suitability
765 trends for species of conservation concern that has real potential to advance future species and
766 habitat conservation activities.

767 For example, New Mexico, only one of the states occupied by Cassin's Sparrow, is home
768 to more than 5,800 species, about 235 of which have been identified as Species of Greatest
769 Conservation Need [9,180,181]. In the current study, we looked at only one species. Even here,
770 with only 30 and 19 variables respectively in the M2 and MC working set collections, at 100
771 samples per variable performed in triplicate, MERRA/Max selection across the two time series
772 required 7,350 independent bivariate sampling runs and a total run time of about 90 minutes in
773 our 100-core testbed. Run time on a single processor for this computational load would have
774 been about four days. In theory, selection would require less than one minute in a fully

775 provisioned 7,350-core cluster computing environment, which makes an otherwise intractable
776 manual analysis possible and perhaps even scalable to accommodate comprehensive, state-level
777 analysis of hundreds of species. It is not unreasonable to imagine a fully realized, operational
778 implementation of this analytic workflow being made available to the research community on a
779 cost-effective basis through one of many commercial cloud services [182–187].

780 There are methodological details in the current study that could raise concern, many of
781 which we hope to address as our work in this area progresses. For example, we started with birds
782 because of the ready access to historical, georeferenced occurrence and survey data on birds that
783 are available through resources such as GBIF and USGS's BBS. Application programming
784 interfaces (APIs) and R libraries are making these resources increasingly easy to work with, but
785 the vetting of observations, winnowing of records, and otherwise perfecting of ENM inputs
786 remains a science based largely on expert knowledge, subject to controversy, and difficult to
787 automate. Our default settings seem to work well for our purposes [74], but could be inadequate
788 for other applications. It will be a challenge to extend this approach to organisms lacking the
789 abundant, publicly-accessible observational records that are currently available for birds.

790 We are sometimes criticized for using reanalysis data for ENM studies, generally by
791 numerical climate modelers who value reanalyses for different reasons and have reservations
792 about using the data in other applications. Their concerns usually revolve around the potential
793 biases or errors that might exist in what are primarily research datasets. However, we still see
794 untapped value in these data because of their diversity of modeled attributes, the way reanalyses
795 integrate such a wide range of Earth system measurements, and their remarkably high temporal
796 resolution, which opens doors to a level of temporally fine-grained analysis difficult to obtain
797 with other types of data. Furthermore, our focus is on the long-running patterns and trends in

798 environmental drivers, which tend to accommodate bias and resolution issues that may pose
799 problems in applications that rely on actual values from reanalysis datasets.

800 Attitudes appear to be evolving on this issue. For example, Copernicus, the Earth
801 observation component of the European Union's space program, now provides a suite of API-
802 accessible, downscaled reanalysis and projection data products targeted for and vetted by the
803 biodiversity research community [25,188–191]. Copernicus's Climate Data Store [188] will
804 make this type of work far more accessible, and the ability to anchor climatic suitability
805 projections along a continuum that extends from historical trends to the future within a consistent
806 information space could contribute an important new level of insight to conservation status
807 assessments.

808 From a science perspective, the most significant limitation of the current work is that, at
809 this point, it raises more questions than it answers. The ambiguities and uncertainties regarding
810 the conservation status of Cassin's Sparrow that inspired the project in the first place remain
811 unresolved. However, these unanswered questions have helped us identify the key issues to be
812 addressed in next steps. Four areas stand out as being particularly promising topics for future
813 research. The first two directly address the ambiguities question; pursuing them will undoubtedly
814 lead to useful insights into the natural history of Cassin's Sparrow:

815 (1) *State-level conservation status.* Given the variability we observed in climatic
816 suitability across Cassin's Sparrow's range, along with the disparities noted
817 between suitability- and abundance-derived perspectives of this species'
818 status, an updated, state-by-state look at the species' distribution and
819 conservation status is needed in order to better understand regional
820 vulnerabilities and patterns of change. Such an exercise would also be an

821 opportunity to examine the potential of deriving a useful climate change risk
822 metric from retrospective ENM trends that could improve species
823 vulnerability assessments across taxa [7,192–195].

824 (2) *Interannual variability.* Given the variability we observed in climatic
825 suitability across areas occupied by Cassin's Sparrow during the breeding
826 season, a closer look at the nature and scope of historical, interannual range
827 changes is need. Combining M2 and MC predictors while separating breeding
828 and non-breeding occurrences into monthly time series could potentially
829 identify life-cycle-specific drivers influencing this variability and provide
830 useful insights into the species' itinerant breeding habit, recruitment, dispersal,
831 and overall response to seasonal rainfall and surface wind speed patterns. It
832 would also help address the open research questions raised by points (2) and
833 (3) in the discussion.

834 The next two topics are research questions that have grown out of the current work.
835 While rooted in our interest in Cassin's Sparrow, insights gained through exploration of these
836 topics would likely be more generally applicable across species:

837 (3) *Bridging the correlative-mechanistic (CM) divide.* Correlative ENM focuses
838 on understanding the occurrence-based environmental associations that allow
839 persistence of a species' population; mechanistic modeling seeks to do the
840 same, but based on first principles of biophysics and physiology [196]. The
841 mechanistic links between climate and the environmental responses of an
842 organism occur through the microclimatic conditions that organisms
843 experience on the ground [51]. A growing body of work attests to the value of

844 including biologically-relevant microclimatic variables alongside traditional,
845 macroclimatic drivers in ENM [30,43,49,61,174,175], the practical upshot of
846 which is improved results that blend the best of correlative and mechanistic
847 insight [51,52,197–200]. A major challenge to doing so, however, has been
848 the paucity of detailed knowledge about most organisms' microclimatic and
849 functional requirements, which are needed to parameterize mechanistic
850 models [49,196–198,201]. That challenge notwithstanding, there appears to be
851 little dispute about the types of drivers that represent microclimatic conditions
852 of importance for a diversity of species: they include data on soil properties,
853 wind speed, solar radiation, humidity, cloud cover, etc., essentially a subset of
854 the M2 collection [51,196].

855 In the current study, we are struck by the apparent capacity of reanalysis
856 data plus time-specific variable selection across a retrospective time series to
857 simultaneously identify meaningful macroclimatic variables, microclimatic
858 variables, and variables representing ecological function. This observation
859 suggests the possibility that the approach we have taken here is a step toward
860 bridging the CM divide. Given that Cassin's Sparrow is one of a relatively
861 small group of birds for which the mechanistic drivers behind many
862 behavioral traits have been studied [17], the species could provide a useful
863 focus for examining this issue further.

864 (4) *Bridging the abundance-suitability (AS) divide.* We are intrigued by the
865 apparent congruence between our centroid results and those of Huang et al.
866 [124]: the velocity and direction of shifts in climatic suitability observed by

867 Huang and his colleagues parallels the patterns we observed in our MC
868 results; the velocity and direction of shifts in abundance observed by Huang
869 parallels the results we observed in our M2 results. The similarities raise the
870 question, in our minds, of whether reanalysis-based, retrospective
871 environmental suitability analyses that combine both time-specificity and
872 variable-specificity, as we have done in this study, might provide a practical
873 means of estimating abundance distributions at scale using readily-available
874 occurrence data. Work on this question would help address the open research
875 question raised by point (3) of the discussion above as well as advance the
876 management-relevant benefits suggested by point (4) of the discussion.

877 Finally, a pragmatic next step that will be important in order to address these research
878 topics and enable the approach we have used here to become more generally applicable. We have
879 essentially been exploring the capacity of automated, retrospective ENM to provide a new and
880 useful dimension to studies of the temporal dynamics of climatic suitability. To gain experience
881 and confidence with retrospective ENM, broader community engagement with these methods is
882 needed. To that end, we have begun making the software and data supporting this research
883 available as the MMX Toolkit [202]. We see continued development of the MMX Toolkit,
884 accompanied by community contributions and refinement and feedback on work such as that
885 described here, as key to maturing the methodology, making it truly useful to wildlife
886 conservation activities, and increasing what we know about the current status of Cassin's
887 Sparrow and what the future might hold for this and other species.

888 Literature Cited

- 889 1. Woodhouse SW. *Zonotrichia Cassinii*, nobis. Proceedings of the Academy of Natural
890 Science of Philadelphia. Philadelphia: Merrihow and Thompson; 1852. pp. 60–61.
891 Available: <https://www.biodiversitylibrary.org/item/17888#page/7/mode/1up>
- 892 2. Dunning, Jr. JB, Bowers, Jr. RK, Suter SJ, Bock CE. Cassin's Sparrow (*Peucaea cassini*),
893 Version 1.0. In: Birds of the World (P. G. Rodewald, Editor) [Internet]. 2020 [cited 23 Dec
894 2022]. Available: <https://doi.org/10.2173/bow.casspa.01>
- 895 3. Williams FC, LeSassier AL. Cassin's Sparrow. In: Austin OL, editor. Life Histories of
896 North American Cardinals, Grosbeaks, Buntings, Towhees, Finches, Sparrows, and Allies,
897 Order Passeriformes, Family Fringillidae: (in 3vols) Part 2, Genera *Pipilo* (part) Through
898 *Spizella*. New York: Dover; 1968. pp. 981–990.
- 899 4. Iknayan KJ, Beissinger SR. Collapse of a desert bird community over the past century
900 driven by climate change. Proc Natl Acad Sci USA. 2018;115: 8597.
901 doi:10.1073/pnas.1805123115
- 902 5. Ruth JM. Cassin's Sparrow (*Aimophila cassinii*) status assessment and conservation plan.
903 Denver, CO; 2000. Report No.: BTP-R6002-2000. Available:
904 <http://pubs.er.usgs.gov/publication/2002055>
- 905 6. Wolf B. Global warming and avian occupancy of hot deserts; a physiological and
906 behavioral perspective. Revista Chilena de Historia Natural. 2000;73: 395–400.

- 907 7. Wilsey C, Taylor L, Bateman B, Jensen C, Michel N, Panjabi A, et al. Climate policy
908 action needed to reduce vulnerability of conservation-reliant grassland birds in North
909 America. Conservat Sci and Prac. 2019;1. doi:10.1111/csp2.21
- 910 8. Bateman BL, Pidgeon AM, Radeloff VC, VanDerWal J, Thogmartin WE, Vavrus SJ, et al.
911 The pace of past climate change vs. potential bird distributions and land use in the United
912 States. Global Change Biology. 2016;22: 1130–1144. doi:10.1111/gcb.13154
- 913 9. Game NM, Fish. New Mexico State Wildlife Action Plan (SWAP) Final 2019. In: New
914 Mexico Department of Game & Fish [Internet]. 2019 [cited 16 Oct 2022]. Available:
915 [https://www.wildlife.state.nm.us/wpfb-file/new-mexico-state-wildlife-action-plan-swap-](https://www.wildlife.state.nm.us/wpfb-file/new-mexico-state-wildlife-action-plan-swap-final-2019-pdf/)
916 [final-2019-pdf/](https://www.wildlife.state.nm.us/wpfb-file/new-mexico-state-wildlife-action-plan-swap-final-2019-pdf/)
- 917 10. Cassin's Sparrow - Whatbird.com. [cited 22 May 2021]. Available:
918 https://identify.whatbird.com/obj/278/overview/cassins_sparrow.aspx
- 919 11. Cassin's Sparrow. In: Audubon [Internet]. 2014 [cited 22 May 2021]. Available:
920 <https://www.audubon.org/field-guide/bird/cassins-sparrow>
- 921 12. Cassin's Sparrow (*Peucaea cassinii*) - BirdLife species factsheet. [cited 22 May 2021].
922 Available: <http://datazone.birdlife.org/species/factsheet/22721272>
- 923 13. Cassin's Sparrow Life History, All About Birds, Cornell Lab of Ornithology. [cited 22 May
924 2021]. Available: https://www.allaboutbirds.org/guide/Cassins_Sparrow/lifehistory
- 925 14. New Mexico Avian Conservation Partners | NMACP. [cited 7 Oct 2022]. Available:
926 <https://avianconservationpartners-nm.org/>
- 927 15. Salas EAL, Seamster VA, Boykin KG, Harings NM, Dixon KW, Department of Fish,
928 Wildlife and Conservation Ecology, New Mexico State University, Las Cruces, New

- 929 Mexico 88003, USA. Modeling the impacts of climate change on Species of Concern
930 (birds) in South Central U.S. based on bioclimatic variables. AIMS Environmental Science.
931 2017;4: 358–385. doi:10.3934/environsci.2017.2.358
- 932 16. *Peucaea cassinii* | NatureServe Explorer. [cited 16 Jun 2023]. Available:
933 https://explorer.natureserve.org/Taxon/ELEMENT_GLOBAL.2.102862/Peucaea_cassinii
- 934 17. Schnase JL, Grant WE, Maxwell TC, Leggett JJ. Time and energy budgets of Cassin's
935 sparrow (*Aimophila cassinii*) during the breeding season: evaluation through modelling.
936 Ecological Modelling. 1991;55: 285–319.
- 937 18. Lynn J. Cassin's Sparrow (*Aimophila cassinii*): A Technical Conservation Assessment.
938 USDA Forest Service; 2006. Available:
939 http://www.fs.usda.gov/Internet/FSE_DOCUMENTS/stelprdb5182053.pdf
- 940 19. Maxwell TC. Avifauna of the Concho Valley of West-Central Texas with Special
941 Reference to Historical Change. Texas A&M University. 1979.
- 942 20. Ohmart RD. Dual breeding ranges in Cassin's sparrow (*Aimophila cassinii*). In: Hoff CC,
943 Riedesel ML, editors. Physiological systems in semiarid environments. Albuquerque, NM:
944 University of New Mexico Press; 1969. p. 105.
- 945 21. Schnase JL, Maxwell TC. Use of song patterns to identify individual male Cassin's
946 Sparrows. Journal of Field Ornithology. 1989;60: 12–19.
- 947 22. Maguire Jr B. Niche response structure and the analytical potentials of its relationship to
948 the habitat. The American Naturalist. 1973;107: 213–246.

- 949 23. Pecl GT, Araújo MB, Bell JD, Blanchard J, Bonebrake TC, Chen I-C, et al. Biodiversity
950 redistribution under climate change: Impacts on ecosystems and human well-being.
951 Science. 2017;355: eaai9214. doi:10.1126/science.aai9214
- 952 24. Johnston A, Auer T, Fink D, Strimas-Mackey M, Iliff M, Rosenberg KV, et al. Comparing
953 abundance distributions and range maps in spatial conservation planning for migratory
954 species. Ecol Appl. 2020;30. doi:10.1002/eap.2058
- 955 25. Climate reanalysis | Copernicus. [cited 15 Oct 2022]. Available:
956 <https://climate.copernicus.eu/climate-reanalysis>
- 957 26. Edwards PN. A Vast Machine: Computer Models, Climate Data, and the Politics of Global
958 Warming. Cambridge, MA: MIT Press; 2010.
- 959 27. Cavanagh RD, Murphy EJ, Bracegirdle TJ, Turner J, Knowland CA, Corney SP, et al. A
960 Synergistic Approach for Evaluating Climate Model Output for Ecological Applications.
961 Frontiers in Marine Science. 2017;4: 308. doi:10.3389/fmars.2017.00308
- 962 28. Araújo MB, Anderson RP, Barbosa AM, Beale CM, Dormann CF, Early R, et al. Standards
963 for distribution models in biodiversity assessments. Science Advances. 2019;5: eaat4858.
- 964 29. Barbet-Massin M, Jetz W. A 40-year, continent-wide, multispecies assessment of relevant
965 climate predictors for species distribution modelling. Heikkinen R, editor. Diversity and
966 Distributions. 2014;20: 1285–1295. doi:10.1111/ddi.12229
- 967 30. Leitão PJ, Santos MJ. Improving models of species ecological niches: A remote sensing
968 overview. Front Ecol Evol. 2019;7: 9. doi:10.3389/fevo.2019.00009

- 969 31. Simões MVP, Peterson AT. Importance of biotic predictors in estimation of potential
970 invasive areas: the example of the tortoise beetle *Eurypedus nigrosignatus*, in Hispaniola.
971 PeerJ. 2018;6: e6052. doi:10.7717/peerj.6052
- 972 32. Petitpierre B, Broennimann O, Kueffer C, Daehler C, Guisan A. Selecting predictors to
973 maximize the transferability of species distribution models: lessons from cross-continental
974 plant invasions: Which predictors increase the transferability of SDMs? Global Ecology
975 and Biogeography. 2017;26: 275–287. doi:10.1111/geb.12530
- 976 33. Austin MP, Van Niel KP. Improving species distribution models for climate change
977 studies: variable selection and scale: Species distribution models for climate change
978 studies. Journal of Biogeography. 2011;38: 1–8. doi:10.1111/j.1365-2699.2010.02416.x
- 979 34. Bosilovich MG, Lucchesi R, Suarez M. MERRA-2: File Specification. GMAO Office
980 Note. 2016;9: 1–73.
- 981 35. Gelaro R, McCarty W, Su MJ, Todling R, Molod A, Takacs L, et al. The Modern-Era
982 Retrospective Analysis for Research and Applications, Version 2 (MERRA-2). JOURNAL
983 OF CLIMATE. 2017;30: 36.
- 984 36. Fick SE, Hijmans RJ. WorldClim 2: new 1-km spatial resolution climate surfaces for global
985 land areas. International Journal of Climatology. 2017;37: 4302–4315.
986 doi:10.1002/joc.5086
- 987 37. Worldclim bioclimatic variables. 2020 [cited 22 May 2020]. Available:
988 <https://worldclim.org/data/worldclim21.html>
- 989 38. Beaumont LJ, Hughes L, Poulsen M. Predicting species distributions: use of climatic
990 parameters in BIOCLIM and its impact on predictions of species' current and future

- 991 distributions. Ecological Modelling. 2005;186: 251–270.
- 992 doi:10.1016/j.ecolmodel.2005.01.030
- 993 39. Booth TH, Nix HA, Busby JR, Hutchinson MF. BIOCLIM: the first species distribution
994 modelling package, its early applications and relevance to most current MaxEnt studies.
995 Franklin J, editor. Diversity Distrib. 2014;20: 1–9. doi:10.1111/ddi.12144
- 996 40. Hijmans RJ, Cameron SE, Parra JL, Jones PG, Jarvis A. Very high resolution interpolated
997 climate surfaces for global land areas. International Journal of Climatology. 2005;25:
998 1965–1978. doi:10.1002/joc.1276
- 999 41. O'Donnell MS, Ignizio D a. Bioclimatic Predictors for Supporting Ecological Applications
1000 in the Conterminous United States. Reston, VA: US Geological Survey; 2012 p. 10. Report
1001 No.: 691. Available: <https://pubs.usgs.gov/ds/691/>
- 1002 42. Vega GC, Perttierra LR, Olalla-Tárraga MÁ. Data from: MERRAclim, a high-resolution
1003 global dataset of remotely sensed bioclimatic variables for ecological modelling. Dryad;
1004 2018. p. 8324359732 bytes. doi:10.5061/DRYAD.S2V81
- 1005 43. Cabello J, Fernández N, Alcaraz-Segura D, Oyonarte C, Piñeiro G, Altesor A, et al. The
1006 ecosystem functioning dimension in conservation: insights from remote sensing. Biodivers
1007 Conserv. 2012;21: 3287–3305. doi:10.1007/s10531-012-0370-7
- 1008 44. Porzig EL, Seavy NE, Gardali T, Geupel GR, Holyoak M, Eadie JM. Habitat suitability
1009 through time: using time series and habitat models to understand changes in bird density.
1010 Ecosphere. 2014;5: art12. doi:10.1890/ES13-00166.1
- 1011 45. Gonçalves J, Alves P, Pôças I, Marcos B, Sousa-Silva R, Lomba Â, et al. Exploring the
1012 spatiotemporal dynamics of habitat suitability to improve conservation management of a

- 1013 vulnerable plant species. *Biodivers Conserv.* 2016;25: 2867–2888. doi:10.1007/s10531-
1014 016-1206-7

1015 46. Brooks TM, Pimm SL, Akçakaya HR, Buchanan GM, Butchart SHM, Foden W, et al.
1016 Measuring terrestrial area of habitat (AOH) and its utility for the IUCN Red List. *Trends in
1017 Ecology & Evolution.* 2019;34: 977–986. doi:10.1016/j.tree.2019.06.009

1018 47. Oeser J, Heurich M, Senf C, Pflugmacher D, Belotti E, Kuemmerle T. Habitat metrics
1019 based on multi-temporal Landsat imagery for mapping large mammal habitat. Pettorelli N,
1020 Armenteras D, editors. *Remote Sens Ecol Conserv.* 2020;6: 52–69. doi:10.1002/rse2.122

1021 48. Regos A, Gómez-Rodríguez P, Arenas-Castro S, Tapia L, Vidal M, Domínguez J. Model-
1022 assisted bird monitoring based on remotely sensed ecosystem functioning and atlas data.
1023 *Remote Sensing.* 2020;12: 2549. doi:10.3390/rs12162549

1024 49. Regos A, Gonçalves J, Arenas-Castro S, Alcaraz-Segura D, Guisan A, Honrado JP.
1025 Mainstreaming remotely sensed ecosystem functioning in ecological niche models. He K,
1026 Moat J, editors. *Remote Sens Ecol Conserv.* 2022;8: 431–447. doi:10.1002/rse2.255

1027 50. Arenas-Castro S, Sillero N. Cross-scale monitoring of habitat suitability changes using
1028 satellite time series and ecological niche models. *Science of The Total Environment.*
1029 2021;784: 147172. doi:10.1016/j.scitotenv.2021.147172

1030 51. Kearney MR, Isaac AP, Porter WP. microclim: Global estimates of hourly microclimate
1031 based on long-term monthly climate averages. *Sci Data.* 2014;1: 140006.
1032 doi:10.1038/sdata.2014.6

- 1033 52. Kearney M, Simpson SJ, Raubenheimer D, Helmuth B. Modelling the ecological niche
1034 from functional traits. *Phil Trans R Soc B*. 2010;365: 3469–3483.
1035 doi:10.1098/rstb.2010.0034
- 1036 53. Lembrechts JJ, Nijs I, Lenoir J. Incorporating microclimate into species distribution
1037 models. *Ecography*. 2019;42: 1267–1279. doi:10.1111/ecog.03947
- 1038 54. Guisan A, Tingley R, Baumgartner JB, Naujokaitis-Lewis I, Sutcliffe PR, Tulloch AIT, et
1039 al. Predicting species distributions for conservation decisions. Arita H, editor. *Ecol Lett*.
1040 2013;16: 1424–1435. doi:10.1111/ele.12189
- 1041 55. Ingenloff K, Peterson AT. Incorporating time into the traditional correlational distributional
1042 modelling framework: A proof-of-concept using the Wood Thrush *Hylocichla mustelina*.
1043 Peres-Neto P, editor. *Methods Ecol Evol*. 2021;12: 311–321. doi:10.1111/2041-
1044 210X.13523
- 1045 56. Rollinson CR, Finley AO, Alexander MR, Banerjee S, Dixon Hamil K-A, Koenig LE, et al.
1046 Working across space and time: nonstationarity in ecological research and application.
1047 *Front Ecol Environ*. 2021;19: 66–72. doi:10.1002/fee.2298
- 1048 57. Bede-Fazekas Á, Somodi I. The way bioclimatic variables are calculated has impact on
1049 potential distribution models. Freckleton R, editor. *Methods Ecol Evol*. 2020;11: 1559–
1050 1570. doi:10.1111/2041-210X.13488
- 1051 58. Ingenloff K, Hensz CM, Anamza T, Barve V, Campbell LP, Cooper JC, et al. Predictable
1052 invasion dynamics in North American populations of the Eurasian collared dove
1053 *Streptopelia decaocto*. *Proc R Soc B*. 2017;284: 20171157. doi:10.1098/rspb.2017.1157

- 1054 59. Peterson AT, Martínez-Campos C, Nakazawa Y, Martínez-Meyer E. Time-specific
1055 ecological niche modeling predicts spatial dynamics of vector insects and human dengue
1056 cases. *Transactions of The Royal Society of Tropical Medicine and Hygiene*. 2005;99:
1057 647–655. doi:10.1016/j.trstmh.2005.02.004
- 1058 60. Ingenloff K. Enhancing the correlative ecological niche modeling framework to incorporate
1059 the temporal dimension of species' distributions. University of Kansas. 2020.
- 1060 61. Barve N, Martin C, Brunsell NA, Peterson AT. The role of physiological optima in shaping
1061 the geographic distribution of Spanish moss: Physiological optima of Spanish moss. *Global
1062 Ecology and Biogeography*. 2014;23: 633–645. doi:10.1111/geb.12150
- 1063 62. Roubicek AJ, VanDerWal J, Beaumont LJ, Pitman AJ, Wilson P, Hughes L. Does the
1064 choice of climate baseline matter in ecological niche modelling? *Ecological Modelling*.
1065 2010;221: 2280–2286. doi:10.1016/j.ecolmodel.2010.06.021
- 1066 63. Harris RMB, Grose MR, Lee G, Bindoff NL, Porfirio LL, Fox-Hughes P. Climate
1067 projections for ecologists. *Wiley Interdisciplinary Reviews: Climate Change*. 2014;5: 621–
1068 637. doi:10.1002/wcc.291
- 1069 64. Goberville E, Beaugrand G, Hautekèete N-C, Piquot Y, Luczak C. Uncertainties in the
1070 projection of species distributions related to general circulation models. *Ecol Evol*. 2015;5:
1071 1100–1116. doi:10.1002/ece3.1411
- 1072 65. Pérez-Navarro MA, Broennimann O, Esteve MA, Moya-Perez JM, Carreño MF, Guisan A,
1073 et al. Temporal variability is key to modelling the climatic niche. *Diversity and
1074 Distributions*. 2021;27: 473–484. doi:10.1111/ddi.13207

- 1075 66. Guida RJ, Abella SR, Jr WJS, Stephen H, Roberts CL. Climatic change and desert
1076 vegetation distribution: Assessing thirty years of change in southern nevada's Mojave
1077 Desert. *The Professional Geographer*. 2014;66: 311–322.
1078 doi:10.1080/00330124.2013.787007
- 1079 67. Guida RJ, Abella SR, Roberts CL, Norman CM, Smith Jr. WJ. Assessing historical and
1080 future habitat models for four conservation-priority Mojave Desert species. *Journal of
1081 Biogeography*. 2019;46: 2081–2097. doi:<https://doi.org/10.1111/jbi.13645>
- 1082 68. Araújo MB, Guisan A. Five (or so) challenges for species distribution modelling. *Journal of
1083 Biogeography*. 2006;33: 1677–1688. doi:10.1111/j.1365-2699.2006.01584.x
- 1084 69. Smith AB, Santos MJ. Testing the ability of species distribution models to infer variable
1085 importance. *Ecography*. 2020;43: 1801–1813. doi:10.1111/ecog.05317
- 1086 70. Cobos ME, Peterson AT, Osorio-Olvera L, Jiménez-García D. An exhaustive analysis of
1087 heuristic methods for variable selection in ecological niche modeling and species
1088 distribution modeling. *Ecological Informatics*. 2019;53: 100983.
1089 doi:10.1016/j.ecoinf.2019.100983
- 1090 71. Peterson AT, Cobos ME, Jiménez-García D. Major challenges for correlational ecological
1091 niche model projections to future climate conditions: Climate change, ecological niche
1092 models, and uncertainty. *Annals of the New York Academy of Sciences*. 2018;1429: 66–
1093 77. doi:10.1111/nyas.13873
- 1094 72. Peterson AT, Nakazawa Y. Environmental data sets matter in ecological niche modelling:
1095 an example with *Solenopsis invicta* and *Solenopsis richteri*. *Global Ecology and
1096 Biogeography*. 2008;0: 071113201427001-???. doi:10.1111/j.1466-8238.2007.00347.x

- 1097 73. Zeng Y, Low BW, Yeo DCJ. Novel methods to select environmental variables in MaxEnt:
1098 A case study using invasive crayfish. Ecological Modelling. 2016;341: 5–13.
1099 doi:<https://doi.org/10.1016/j.ecolmodel.2016.09.019>
- 1100 74. Schnase JL, Carroll ML. Automatic variable selection in ecological niche modeling: A case
1101 study using Cassin's Sparrow (*Peucaea cassinii*). PLOS ONE. 2022;17: e0257502.
1102 doi:[10.1371/journal.pone.0257502](https://doi.org/10.1371/journal.pone.0257502)
- 1103 75. Schnase JL, Carroll ML, Gill RL, Tamkin GS, Li J, Strong SL, et al. Toward a Monte Carlo
1104 approach to selecting climate variables in MaxEnt. PLOS ONE. 2021;16: e0237208.
1105 doi:[10.1371/journal.pone.0237208](https://doi.org/10.1371/journal.pone.0237208)
- 1106 76. Elith J, Phillips SJ, Hastie T, Dudík M, Chee YE, Yates CJ. A statistical explanation of
1107 MaxEnt for ecologists. Diversity and distributions. 2011;17: 43–57.
- 1108 77. Phillips SJ, Anderson RP, Dudík M, Schapire RE, Blair ME. Opening the black box: An
1109 open-source release of Maxent. Ecography. 2017;40: 887–893.
- 1110 78. Phillips SJ. A Brief Tutorial on Maxent. AT&T Research. 2005;190: 231–259.
- 1111 79. Searcy CA, Shaffer HB. Do ecological niche models accurately identify climatic
1112 determinants of species ranges? The American Naturalist. 2016;187: 423–435.
1113 doi:[10.1086/685387](https://doi.org/10.1086/685387)
- 1114 80. Schnase JL, Carroll ML. The MMX Toolkit: High performance, reanalysis-based climatic
1115 suitability modeling to advance avian conservation. In: Albani S, Lumnitz S, Soille P,
1116 editors. Proceedings of the 2023 conference on Big Data from Space – 6–9 November 2023.
1117 Vienna: European Commission, Joint Research Centre, Publications Office; 2023. (to
1118 appear)

- 1119 81. Chamberlain S, Oldoni D, Barve V, Desmet P, Geffert L, Mcglinn D, et al. rgbif: Interface
1120 to the Global Biodiversity Information Facility API. 2022. Available: [https://CRAN.R-
1121 project.org/package=rgbif](https://CRAN.R-project.org/package=rgbif)
- 1122 82. GBIF - Global Biodiversity Information Facility. 2023 [cited 14 Aug 2023]. Available:
1123 <https://www.gbif.org/>
- 1124 83. Cassin's Sparrow - eBird. [cited 5 Feb 2022]. Available: <https://ebird.org/species/casspa>
- 1125 84. iNaturalist. In: iNaturalist [Internet]. [cited 6 Oct 2022]. Available:
1126 <https://www.inaturalist.org/>
- 1127 85. Data and Samples | NSF NEON | Open Data to Understand our Ecosystems. [cited 26 Dec
1128 2022]. Available: <https://www.neonscience.org/data-samples>
- 1129 86. Smithsonian National Museum of Natural History. [cited 26 Dec 2022]. Available:
1130 <https://naturalhistory.si.edu/>
- 1131 87. Department of Ornithology | AMNH. In: American Museum of Natural History [Internet].
1132 [cited 26 Dec 2022]. Available: [https://bigbangblocks.amnh.org/research/vertebrate-
zoology/ornithology](https://bigbangblocks.amnh.org/research/vertebrate-
1133 zoology/ornithology)
- 1134 88. Museum of Comparative Zoology. [cited 26 Dec 2022]. Available:
1135 <https://mcz.harvard.edu/home>
- 1136 89. Snow FH. Catalogue of the Birds of Kansas. Transactions of the Kansas Academy of
1137 Science (1872-1880). 1872;1: 21–29. doi:10.2307/3623510
- 1138 90. University of Arizona Museum of Natural History. [cited 26 Dec 2022]. Available:
1139 <http://eebweb.arizona.edu/Collections/>

- 1140 91. Boria RA, Blois JL. The effect of large sample sizes on ecological niche models: Analysis
1141 using a North American rodent, *Peromyscus maniculatus*. Ecological Modelling. 2018;386:
1142 83–88. doi:<https://doi.org/10.1016/j.ecolmodel.2018.08.013>
- 1143 92. Boria RA, Olson LE, Goodman SM, Anderson RP. Spatial filtering to reduce sampling bias
1144 can improve the performance of ecological niche models. Ecological Modelling. 2014;275:
1145 73–77. doi:[10.1016/j.ecolmodel.2013.12.012](https://doi.org/10.1016/j.ecolmodel.2013.12.012)
- 1146 93. Sillero N, Barbosa AM. Common mistakes in ecological niche models. International
1147 Journal of Geographical Information Science. 2021;35: 213–226.
1148 doi:[10.1080/13658816.2020.1798968](https://doi.org/10.1080/13658816.2020.1798968)
- 1149 94. Kramer-Schadt S, Niedballa J, Pilgrim JD, Schröder B, Lindenborn J, Reinfelder V, et al.
1150 The importance of correcting for sampling bias in MaxEnt species distribution models.
1151 Robertson M, editor. Diversity Distrib. 2013;19: 1366–1379. doi:[10.1111/ddi.12096](https://doi.org/10.1111/ddi.12096)
- 1152 95. Gap Analysis Project | U.S. Geological Survey. [cited 10 Oct 2022]. Available:
1153 <https://www.usgs.gov/programs/gap-analysis-project>
- 1154 96. Reichle RH. The MERRA-Land Data Product. GMAO Office Note No 3 (Version 12).
1155 2012; 38.
- 1156 97. NASA Center for Climate Simulation | High Performance Computing for Science. [cited 6
1157 Oct 2022]. Available: <https://www.nccs.nasa.gov/>
- 1158 98. GES DISC - Goddard Earth Science Data and Information Services Center. [cited 26 May
1159 2021]. Available: <https://disc.gsfc.nasa.gov/>
- 1160 99. GES DISC Tools: MERRA Subsetter. [cited 6 Oct 2022]. Available:
1161 <https://disc.gsfc.nasa.gov/information/tools?title=MERRA%20Subsetter>

- 1162 100. Hoyer S, Hamman JJ. xarray: N-D labeled Arrays and Datasets in Python. *Journal of Open*
1163 *Research Software*. 2017;5: 10. doi:10.5334/jors.148
- 1164 101. GDAL/OGR Geospatial Data Abstraction Software Library. Open Source Geospatial
1165 Foundation; 2020. Available: <https://gdal.org/>
- 1166 102. Hijmans RJ, Phillips S, Elith J, Leathwick J. dismo: Species Distribution Modeling. 2017.
1167 Available: <https://CRAN.R-project.org/package=dismo>
- 1168 103. Hijmans RJ, Etten J van, Sumner M, Cheng J, Baston D, Bevan A, et al. raster: Geographic
1169 Data Analysis and Modeling. 2022. Available: <https://CRAN.R-project.org/package=raster>
- 1170 104. Hijmans RJ, Phillips S, Elith JL and J. dismo: Species Distribution Modeling. 2022.
1171 Available: <https://CRAN.R-project.org/package=dismo>
- 1172 105. C. Vega G, Pertierra LR, Olalla-Tárraga MÁ. MERRAclim, a high-resolution global
1173 dataset of remotely sensed bioclimatic variables for ecological modelling. *Scientific Data*.
1174 2017;4. doi:10.1038/sdata.2017.78
- 1175 106. Reichle RH, Liu Q, Koster RD, Draper CS, Mahanama SPP, Partyka GS. Land surface
1176 precipitation in MERRA-2. *Journal of Climate*. 2017;30: 1643–1664. doi:10.1175/JCLI-D-
1177 16-0570.1
- 1178 107. Explore | NASA Center for Climate Simulation. [cited 17 Oct 2022]. Available:
1179 <https://www.nccs.nasa.gov/systems/ADAPT>
- 1180 108. Pradhan P. Strengthening MaxEnt modelling through screening of redundant explanatory
1181 bioclimatic variables with variance inflation factor analysis. *Researcher*. 2016;8: 29–34.
- 1182 109. Naimi B. usdm: Uncertainty Analysis for Species Distribution Models. 2017. Available:
1183 <https://CRAN.R-project.org/package=usdm>

- 1184 110. Muscarella R, Galante PJ, Soley-Guardia M, Boria RA, Kass JM, Uriarte M, et al.
1185 ENMeval: An R package for conducting spatially independent evaluations and estimating
1186 optimal model complexity for Maxent ecological niche models. Methods in Ecology and
1187 Evolution. 2014;5: 1198–1205. doi:10.1111/2041-210X.12261
- 1188 111. Kass JM, Muscarella R, Galante PJ, Bohl C, Buitrago-Pinilla GE, Boria RA, et al.
1189 ENMeval: Automated Tuning and Evaluations of Ecological Niche Models. 2022.
1190 Available: <https://CRAN.R-project.org/package=ENMeval>
- 1191 112. mrmmaxent. Maxent. 2022. Available: <https://github.com/mrmmaxent/Maxent>
- 1192 113. Phillips S. A Brief Tutorial on Maxent. 2010; 29.
- 1193 114. H. Akaike. A new look at the statistical model identification. IEEE Transactions on
1194 Automatic Control. 1974;19: 716–723. doi:10.1109/TAC.1974.1100705
- 1195 115. Phillips SJ, Anderson RP, Schapire RE. Maximum entropy modeling of species geographic
1196 distributions. Ecological Modelling. 2006;190: 231–259.
1197 doi:10.1016/j.ecolmodel.2005.03.026.
- 1198 116. Phillips SJ, Research T. A Brief Tutorial on Maxent. 2017; 39.
- 1199 117. Stephens PA, Mason LR, Green RE, Gregory RD, Sauer JR, Alison J, et al. Consistent
1200 response of bird populations to climate change on two continents. Science. 2016;352: 84–
1201 87. doi:10.1126/science.aac4858
- 1202 118. Sen PK. Estimates of the regression coefficient based on Kendall's tau. Journal of the
1203 American statistical association. 1968;63: 1379–1389.
- 1204 119. Theil H. A rank-invariant method of linear and polynomial regression analysis.
1205 Indagationes mathematicae. 1950;12: 173.

- 1206 120. Siegel AF. Robust regression using repeated medians. *Biometrika*. 1982;69: 242–244.
- 1207 121. Evans JS, Murphy MA, Ram K. *spatialEco*: Spatial Analysis and Modelling Utilities. 2022.
1208 Available: <https://CRAN.R-project.org/package=spatialEco>
- 1209 122. VanDerWal J, Murphy HT, Kutt AS, Perkins GC, Bateman BL, Perry JJ, et al. Focus on
1210 poleward shifts in species' distribution underestimates the fingerprint of climate change.
1211 *Nature Clim Change*. 2013;3: 239–243. doi:10.1038/nclimate1688
- 1212 123. Huang Q, Sauer JR, Swatantran A, Dubayah R. A centroid model of species distribution
1213 with applications to the Carolina wren *Thryothorus ludovicianus* and house finch
1214 *Haemorhous mexicanus* in the United States. *Ecography*. 2016;39: 54–66.
1215 doi:10.1111/ecog.01447
- 1216 124. Huang Q, Bateman BL, Michel NL, Pidgeon AM, Radloff VC, Heglund P, et al. Modeled
1217 distribution shifts of North American birds over four decades based on suitable climate
1218 alone do not predict observed shifts. *Science of The Total Environment*. 2023;857: 159603.
1219 doi:10.1016/j.scitotenv.2022.159603
- 1220 125. La Sorte FA, Jetz W. Tracking of climatic niche boundaries under recent climate change:
1221 Niche tracking under recent climate change. *Journal of Animal Ecology*. 2012;81: 914–
1222 925. doi:10.1111/j.1365-2656.2012.01958.x
- 1223 126. Smith AB. *enmSdmX*: Species Distribution Modeling and Ecological Niche Modeling.
1224 2023. Available: <https://cran.r-project.org/web/packages/enmSdmX/index.html>
- 1225 127. Phillips SJ, Dudík M. Modeling of species distributions with Maxent: new extensions and a
1226 comprehensive evaluation. *Ecography*. 2008;31: 161–175.

- 1227 128. (*Peucaea cassinii*) - Species Map - eBird. 2022 [cited 30 Sep 2022]. Available:
1228 <https://ebird.org/map/casspa>
- 1229 129. Fielding AH, Bell JF. A review of methods for the assessment of prediction errors in
1230 conservation presence/absence models. Environmental Conservation. 1997;24: 38–49.
1231 doi:10.1017/S0376892997000088
- 1232 130. Lobo JM, Jiménez-Valverde A, Real R. AUC: a misleading measure of the performance of
1233 predictive distribution models. Global Ecology and Biogeography. 2007; 7.
- 1234 131. Allouche O, Tsoar A, Kadmon R. Assessing the accuracy of species distribution models:
1235 prevalence, kappa and the true skill statistic (TSS): Assessing the accuracy of distribution
1236 models. Journal of Applied Ecology. 2006;43: 1223–1232. doi:10.1111/j.1365-
1237 2664.2006.01214.x
- 1238 132. Frans VF. True Skill Statistic (TSS) calculation across multiple maxent runs. Michigan
1239 State University; 2018 p. 5.
- 1240 133. Warren DL, Seifert SN. Ecological niche modeling in Maxent: The importance of model
1241 complexity and the performance of model selection criteria. Ecological Applications.
1242 2011;21: 335–342. doi:10.1890/10-1171.1
- 1243 134. Arenas-Castro S, Gonçalves J, Alves P, Alcaraz-Segura D, Honrado JP. Assessing the
1244 multi-scale predictive ability of ecosystem functional attributes for species distribution
1245 modelling. Joseph S, editor. PLoS ONE. 2018;13: e0199292.
1246 doi:10.1371/journal.pone.0199292

- 1247 135. Saunders SP, Michel NL, Bateman BL, Wilsey CB, Dale K, LeBaron GS, et al.
1248 Community science validates climate suitability projections from ecological niche
1249 modeling. *Ecol Appl.* 2020;30. doi:10.1002/eap.2128
- 1250 136. Langham GM, Schuetz JG, Distler T, Soykan CU, Wilsey C. Conservation Status of North
1251 American Birds in the Face of Future Climate Change. LaDeau SL, editor. PLoS ONE.
1252 2015;10: e0135350. doi:10.1371/journal.pone.0135350
- 1253 137. Lehikoinen A, Virkkala R. North by north-west: climate change and directions of density
1254 shifts in birds. *Glob Change Biol.* 2016;22: 1121–1129. doi:10.1111/gcb.13150
- 1255 138. North American Breeding Bird Survey. 2017. Available: <https://www.pwrc.usgs.gov/bbs/>.
- 1256 139. Hubbard JP. The status of Cassin's Sparrow in New Mexico and adjacent states. *American*
1257 *Birds.* 1977;31: 933–941.
- 1258 140. Gillings S, Balmer DE, Fuller RJ. Directionality of recent bird distribution shifts and
1259 climate change in Great Britain. *Global Change Biology.* 2015;21: 2155–2168.
1260 doi:<https://doi.org/10.1111/gcb.12823>
- 1261 141. Bateman BL, Pidgeon AM, Radeloff VC, Flather CH, VanDerWal J, Akçakaya HR, et al.
1262 Potential breeding distributions of U.S. birds predicted with both short-term variability and
1263 long-term average climate data. *Ecological Applications.* 2016;26: 2720–2731.
1264 doi:10.1002/eap.1416
- 1265 142. NatureServe Conservation Status Assessment | NatureServe. [cited 17 Jun 2023].
1266 Available: <https://www.natureserve.org/conservation-status-assessment>
- 1267 143. BBS - USGS Patuxent Wildlife Research Center. [cited 18 Jun 2023]. Available:
1268 <https://www.pwrc.usgs.gov/bbs/>

- 1269 144. USFWS Association of Fish and Wildlife Agencies State Wildlife Action Plans (SWAP):
1270 Home. [cited 18 Jun 2023]. Available: <https://www.fishwildlife.org/afwa-informs/state-wildlife-action-plans>
- 1272 145. Weber MM, Stevens RD, Diniz-Filho JAF, Grelle CEV. Is there a correlation between
1273 abundance and environmental suitability derived from ecological niche modelling? A meta-
1274 analysis. *Ecography*. 2017;40: 817–828. doi:10.1111/ecog.02125
- 1275 146. Dallas TA, Hastings A. Habitat suitability estimated by niche models is largely unrelated to
1276 species abundance. *Global Ecol Biogeogr*. 2018;27: 1448–1456. doi:10.1111/geb.12820
- 1277 147. Schofield LN, Siegel RB, Loffland HL. Modeling climate-driven range shifts in
1278 populations of two bird species limited by habitat independent of climate. *Ecosphere*.
1279 2023;14. doi:10.1002/ecs2.4408
- 1280 148. Cavalcante T, Weber MM, Barnett AA. Combining geospatial abundance and ecological
1281 niche models to identify high-priority areas for conservation: The neglected role of
1282 broadscale interspecific competition. *Front Ecol Evol*. 2022;10: 915325.
1283 doi:10.3389/fevo.2022.915325
- 1284 149. Arroyo B, Estrada A, Casas F, Cardador L, De Cáceres M, Bota G, et al. Functional habitat
1285 suitability and urban encroachment explain temporal and spatial variations in abundance of
1286 a declining farmland bird, the Little Bustard *Tetrax tetrax*. *ACE*. 2022;17: art19.
1287 doi:10.5751/ACE-02243-170219
- 1288 150. Monnier-Corbel A, Robert A, Hingrat Y, Benito BM, Monnet A-C. Species Distribution
1289 Models predict abundance and its temporal variation in a steppe bird population. *Global
1290 Ecology and Conservation*. 2023;43: e02442. doi:10.1016/j.gecco.2023.e02442

- 1291 151. Meehan TD, Michel NL, Rue H. Spatial modeling of Audubon Christmas Bird Counts
1292 reveals fine-scale patterns and drivers of relative abundance trends. *Ecosphere*. 2019;10:
1293 e02707. doi:10.1002/ecs2.2707
- 1294 152. Osorio-Olvera LA, Falconi M, Soberón J. Sobre la relación entre idoneidad del hábitat y la
1295 abundancia poblacional bajo diferentes escenarios de dispersión. *Revista Mexicana de
1296 Biodiversidad*. 2016;87: 1080–1088. doi:10.1016/j.rmb.2016.07.001
- 1297 153. Lunghi E, Manenti R, Mulargia M, Veith M, Corti C, Ficetola GF. Environmental
1298 suitability models predict population density, performance and body condition for
1299 microendemic salamanders. *Sci Rep*. 2018;8: 7527. doi:10.1038/s41598-018-25704-1
- 1300 154. Alcaraz-Segura D, Lomba A, Sousa-Silva R, Nieto-Lugilde D, Alves P, Georges D, et al.
1301 Potential of satellite-derived ecosystem functional attributes to anticipate species range
1302 shifts. *International Journal of Applied Earth Observation and Geoinformation*. 2017;57:
1303 86–92. doi:10.1016/j.jag.2016.12.009
- 1304 155. Bradie J, Leung B. A quantitative synthesis of the importance of variables used in MaxEnt
1305 species distribution models. *Journal of Biogeography*. 2017;44: 1344–1361.
1306 doi:10.1111/jbi.12894
- 1307 156. Currie DJ, Venne S. Climate change is not a major driver of shifts in the geographical
1308 distributions of North American birds. *Global Ecology and Biogeography*. 2017;26: 333–
1309 346.
- 1310 157. Harris DB, Gregory SD, Brook BW, Ritchie EG, Croft DB, Coulson G, et al. The influence
1311 of non-climate predictors at local and landscape resolutions depends on the autecology of

- 1312 the species: Autecology informs SDM scale and predictor choice. *Austral Ecology*.
1313 2014;39: 710–721. doi:10.1111/aec.12134
- 1314 158. Schnase JL, Carroll ML. MERRA/Max: Harnessing the Potential of Climate Model
1315 Outputs in Studies of Ecosystem Change. *ESA 2020 Virtual Meeting*. ESA; 2020.
1316 Available: <https://eco.confex.com/eco/2020/meetingapp.cgi/Paper/86032>
- 1317 159. Carroll ML, Schnase JL, Gill RL, Tamkin GS, Li J, Maxwell TP, et al. MERRAMax: A
1318 machine learning approach to stochastic convergence with a multi-variate dataset. *IGARSS*
1319 2020 - 2020 IEEE International Geoscience and Remote Sensing Symposium. Waikoloa,
1320 HI, USA: IEEE; 2020. pp. 2017–2020. doi:10.1109/IGARSS39084.2020.9324185
- 1321 160. Carroll ML, Schnase JL. MERRA/Max: A Down-Selection and Monte Carlo Convergence-
1322 Based Modeling of Complex Systems. *AGU Fall Meeting Abstracts*. San Francisco: AGU;
1323 2019. Available: <https://agu.confex.com/agu/fm19/meetingapp.cgi/Paper/496296>
- 1324 161. Stahle DW. Anthropogenic megadrought. *Science*. 2020;368: 238–239.
1325 doi:10.1126/science.abb6902
- 1326 162. Williams AP, Cook ER, Smerdon JE, Cook BI, Abatzoglou JT, Bolles K, et al. Large
1327 contribution from anthropogenic warming to an emerging North American megadrought.
1328 *Science*. 2020;368: 314–318. doi:10.1126/science.aaz9600
- 1329 163. The North American Monsoon | NOAA Climate.gov. 2021 [cited 29 Jun 2023]. Available:
1330 <http://www.climate.gov/news-features/blogs/enso/north-american-monsoon>
- 1331 164. Zeng J, Zhang Q. The trends in land surface heat fluxes over global monsoon domains and
1332 their responses to monsoon and precipitation. *Sci Rep*. 2020;10: 5762. doi:10.1038/s41598-
1333 020-62467-0

- 1334 165. NOAA. The North American Monsoon. NOAA NWS Climate Prediction Center; 2019 p.
- 1335 25. Available: https://www.cpc.ncep.noaa.gov/products/outreach/Report-to-the-Nation-Monsoon_aug04.pdf
- 1337 166. Adams DK, Comrie AC. The North American Monsoon. Bull Amer Meteor Soc. 1997;78:
- 1338 2197–2213. doi:10.1175/1520-0477(1997)078<2197:TNAM>2.0.CO;2
- 1339 167. Liebmann B. Characteristics of North American Summertime Rainfall with Emphasis on
- 1340 the Monsoon. American Meteorological Society Jounal of Climate. 2008;21: 1277–1294.
- 1341 168. Adams DK. Review of Variability in the North American Monsoon. 2016 [cited 1 Jul
- 1342 2023]. Available: <https://geochange.er.usgs.gov/sw/changes/natural/monsoon/>
- 1343 169. Hobeichi S, Abramowitz G, Ukkola AM, De Kauwe M, Pitman A, Evans JP, et al.
- 1344 Reconciling historical changes in the hydrological cycle over land. npj Clim Atmos Sci.
- 1345 2022;5: 17. doi:10.1038/s41612-022-00240-y
- 1346 170. Hamal K, Sharma S, Khadka N, Baniya B, Ali M, Shrestha MS, et al. Evaluation of
- 1347 MERRA-2 Precipitation Products Using Gauge Observation in Nepal. Hydrology. 2020;7:
- 1348 40. doi:10.3390/hydrology7030040
- 1349 171. Lehmann P, Merlin O, Gentine P, Or D. Soil Texture Effects on Surface Resistance to
- 1350 Bare-Soil Evaporation. Geophysical Research Letters. 2018;45.
- 1351 doi:10.1029/2018GL078803
- 1352 172. Lian X, Zhao W, Gentine P. Recent global decline in rainfall interception loss due to
- 1353 altered rainfall regimes. Nat Commun. 2022;13: 7642. doi:10.1038/s41467-022-35414-y

- 1354 173. Cheng Y, Chan PW, Wei X, Hu Z, Kuang Z, McColl KA. Soil Moisture Control of
1355 Precipitation Re-evaporation over a Heterogeneous Land Surface. *Journal of the*
1356 *Atmospheric Sciences*. 2021;78: 3369–3383. doi:10.1175/JAS-D-21-0059.1
- 1357 174. Lortie CJ, Filazzola A, Westphal M, Butterfield HS. Foundation plant species provide
1358 resilience and microclimatic heterogeneity in drylands. *Sci Rep.* 2022;12: 18005.
1359 doi:10.1038/s41598-022-22579-1
- 1360 175. Varner J, Dearing MD. The importance of biologically relevant microclimates in habitat
1361 suitability assessments. Moreau CS, editor. *PLoS ONE*. 2014;9: e104648.
1362 doi:10.1371/journal.pone.0104648
- 1363 176. Porter WP, Budaraju S, Stewart WE, Ramankutty N. Calculating Climate Effects on Birds
1364 and Mammals: Impacts on Biodiversity, Conservation, Population Parameters, and Global
1365 Community Structure. *American Zoologist*. 2000;40: 597–630. doi:10.1668/0003-
1366 1569(2000)040[0597:cceoba]2.0.co;2
- 1367 177. Ruth JM. Cassin's Sparrow Status Assessment and Conservation Plan. *Biological*
1368 *Technical Publication BTP-R6002-2000*. Denver, CO: U.S. Department of the Interior,
1369 Fish and Wildlife Service; 2000.
- 1370 178. Lynn J. Cassin's Sparrow (*Aimophila cassinii*): A Technical Conservation Assessment.
1371 USDA Forest Service, Species Conservation Project. Rocky Mountain Region. 2006;46.
- 1372 179. Anderson JT, Conway WC. The flight song display of the Cassin's Sparrow (*Aimophila*
1373 *cassinii*): form and possible function. *Bulletin of the Texas Ornithological Society*.
1374 2000;33: 1–12.

- 1375 180. New Database available: USGS Releases "Species of Greatest Conservation Need" Lists |
1376 U.S. Geological Survey. [cited 3 Jul 2023]. Available:
1377 <https://www.usgs.gov/news/technical-announcement/new-database-available-usgs-releases-species-greatest-conservation-need>
1378
1379 181. Programs: Fish and Wildlife: Threatened and Endangered: State T&E Data: New Mexico |
1380 Bureau of Land Management. [cited 3 Jul 2023]. Available:
1381 <https://www.blm.gov/programs/fish-and-wildlife/threatened-and-endangered/state-te-data/new-mexico>
1382
1383 182. NASA Case Study – Amazon Web Services (AWS). In: Amazon Web Services, Inc.
1384 [Internet]. 2021 [cited 26 May 2021]. Available:
1385 <https://aws.amazon.com/partners/success/nasa-image-library/>
1386 183. Research and Technical Computing on Amazon Web Services (AWS). In: Amazon Web
1387 Services, Inc. [Internet]. 2021 [cited 26 May 2021]. Available:
1388 <https://aws.amazon.com/government-education/research-and-technical-computing/>
1389 184. Google Cloud offers global support for academic research. In: Google [Internet]. 2019
1390 [cited 26 May 2021]. Available: <https://blog.google/products/google-cloud/google-cloud-offers-global-support-for-academic-research/>
1391
1392 185. Our head's in the cloud, but we're keeping the earth in mind. In: Google Cloud Blog
1393 [Internet]. 2019 [cited 26 May 2021]. Available:
1394 <https://cloud.google.com/blog/topics/google-cloud-next/our-heads-in-the-cloud-but-were-keeping-the-earth-in-mind/>
1395

- 1396 186. Cloud Computing Services | Microsoft Azure. 2021 [cited 26 May 2021]. Available:
1397 <https://azure.microsoft.com/en-us/>
- 1398 187. Data Science Virtual Machines | Microsoft Azure. 2021 [cited 26 May 2021]. Available:
1399 <https://azure.microsoft.com/en-us/services/virtual-machines/data-science-virtual-machines/>
- 1400 188. Copernicus Climate Data Store (CDS). 2021 [cited 8 Nov 2021]. Available:
1401 <https://cds.climate.copernicus.eu/#!/home>
- 1402 189. Copernicus Climate Change Service. Global bioclimatic indicators from 1950 to 2100
1403 derived from climate projections. ECMWF; 2021. doi:10.24381/CDS.A37FECB7
- 1404 190. Copernicus Climate Change Service. Downscaled bioclimatic indicators for selected
1405 regions from 1979 to 2018 derived from reanalysis. ECMWF; 2021.
1406 doi:10.24381/CDS.FE90A594
- 1407 191. About Copernicus | Copernicus. [cited 5 Jul 2023]. Available:
1408 <https://www.copernicus.eu/en/about-copernicus>
- 1409 192. Rinnan DS, Lawler J. Climate-niche factor analysis: a spatial approach to quantifying
1410 species vulnerability to climate change. Ecography. 2019;42: 1494–1503.
1411 doi:10.1111/ecog.03937
- 1412 193. Foden WB, Young BE, Akçakaya HR, Garcia RA, Hoffmann AA, Stein BA, et al. Climate
1413 change vulnerability assessment of species. Wiley interdisciplinary reviews: climate
1414 change. 2019;10: e551.
- 1415 194. Sang Z, Hamann A. Climatic limiting factors of North American ecosystems: a remote-
1416 sensing based vulnerability analysis. Environ Res Lett. 2022;17: 094011.
1417 doi:10.1088/1748-9326/ac8608

- 1418 195. Hatten JR, Giermakowski JT, Holmes JA, Nowak EM, Johnson MJ, Ironside KE, et al.
1419 Identifying bird and reptile vulnerabilities to climate change in the Southwestern United
1420 States. US Geological Survey; 2016.
- 1421 196. Peterson AT, Papeş M, Soberón J. Mechanistic and correlative models of ecological niches.
1422 European Journal of Ecology. 2015;1: 28–38. doi:10.1515/eje-2015-0014
- 1423 197. Dormann CF, Schymanski SJ, Cabral J, Chuine I, Graham C, Hartig F, et al. Correlation
1424 and process in species distribution models: bridging a dichotomy: Bridging the correlation-
1425 process dichotomy. J Biogeogr. 2012;39: 2119–2131. doi:10.1111/j.1365-
1426 2699.2011.02659.x
- 1427 198. Enriquez-Urzelai U, Kearney MR, Nicieza AG, Tingley R. Integrating mechanistic and
1428 correlative niche models to unravel range-limiting processes in a temperate amphibian.
1429 Global Change Biology. 2019;25: 2633–2647. doi:10.1111/gcb.14673
- 1430 199. Evans TG, Diamond SE, Kelly MW. Mechanistic species distribution modelling as a link
1431 between physiology and conservation. Conserv Physiol. 2015;3: cov056.
1432 doi:10.1093/conphys/cov056
- 1433 200. Buckley LB, Urban MC, Angilletta MJ, Crozier LG, Rissler LJ, Sears MW. Can
1434 mechanism inform species' distribution models?: Correlative and mechanistic range
1435 models. Ecology Letters. 2010; no-no. doi:10.1111/j.1461-0248.2010.01479.x
- 1436 201. Van der Meersch V, Chuine I. Estimating process-based model parameters from species
1437 distribution data using the evolutionary algorithm CMA-ES. Methods Ecol Evol. 2023;14:
1438 1808–1820. doi:10.1111/2041-210X.14119

1439 202. Schnase JL, Carroll ML. The MMX Toolkit: High performance, reanalysis-based climatic
1440 suitability modeling to advance avian conservation. Proceedings of the 2023 Conference on
1441 Big Data from Space (BiDS '23). Vienna, Austria; 2023.
1442

Appendix A. MERRA-2 (M2) variable definitions.*

M2T1NXSLV		2D Atmospheric variables
M2-01	TS	Surface skin temperature (K) – <i>An approximation for the temperature of the Earth's tropopause, which lies about 17 km (11 miles) above the surface, expressed in degrees Kelvin. The tropopause is the boundary between the turbulent mixing-dominated troposphere and the more stable stratosphere.</i>
M2-02	QV2M	2-meter specific humidity (kg/kg) – <i>The amount of water vapor contained in a unit amount of air, generally expressed as kg of water per kg of air.</i>
M2-03	T2M	2-meter air temperature (K) – <i>The air temperature 2m above the ground, expressed in degrees Kelvin.</i>
M2T1NXFLX		2D Surface fluxes
M2-04	EFLUX	Positive latent heat flux (W/m ²) – <i>The exchange of energy between the surface of the Earth and the atmosphere when water evaporates from or condenses onto the surface, expressed in Watts per square meter. Positive latent heat flux means that evaporation is occurring.</i>
M2-05	HFLUX	Positive sensible heat flux (W/m ²) – <i>The exchange of energy between the surface of the Earth and the atmosphere when no state change is involved and energy is transferred by conduction, expressed in Watts per square meter. Positive sensible heat flux means heat is flowing from the surface to the atmosphere.</i>
M2-06	SPEED	Surface wind speed (m/s) – <i>The speed of wind flow near the Earth's surface, expressed in meters per second.</i>

* These summaries were derived from definitions provided in: J. R. Holton, J. A. Curry, and J. A. Pyle, Eds., *Encyclopedia of atmospheric sciences*. Amsterdam; Boston: Academic Press, 2003. Details about the MERRA-2 collection and variable naming conventions can be found in: Bosilovich, M.G., R. Lucchesi, and M. Suarez. 2016. “MERRA-2: File Specification.” *GMAO Office Note 9* (Version 1.1): 1–73.

M2-07	PREVTOT	Total re-evaporation/sublimation of precipitation ($\text{kg/m}^2/\text{s}$) – <i>The amount of precipitation that evaporates (water to water vapor transition) or sublimates (snow or ice to water vapor transition) while falling through the atmosphere and fails to arrive at the land surface, expressed in mm per second. [1 kg of water spread over a square meter (kg/m^2) = 1 mm]</i>
M2-08	PRECTOTCORR	Total observation-corrected surface precipitation ($\text{kg/m}^2/\text{s}$) – <i>Total precipitation modeled from atmospheric physics corrected with satellite and/or gauge-based measurements, expressed in mm per second. [1 kg of water spread over a square meter (kg/m^2) = 1 mm]</i>
M2T1NXRAD 2D Surface and top-of-atmosphere radiation fluxes		
M2-09	ALBEDO	Surface albedo – <i>The amount of sunlight reflected by the Earth's surface, generally expressed as a decimal value with 1.0 being a perfect reflector and 0.0 absorbing all incoming light.</i>
M2-10	LWGNT	Surface net downward longwave flux (W/m^2) – <i>The rate of flow of radiant energy reaching the Earth's surface in the thermal infrared spectrum (4-100 μm), expressed in Watts per square meter. LWGNT is a result of atmospheric absorption, emission, and scattering within the entire atmospheric column.</i>
M2-11	SWGNT	Surface net downward shortwave flux (W/m^2) – <i>An estimate of the total amount of shortwave (0.3-4.0 μm) radiative energy that reaches the Earth's surface, expressed in Watts per square meter. An important influence on land-atmosphere and vegetation interactions, SWGNT has many applications in the general and applied sciences.</i>
M2-12	TAUTOT	Optical thickness of all clouds – <i>A measure of attenuation of the light passing through the atmosphere due to the scattering and absorption by cloud droplets. TAUTOT is a dimensionless, monotonically increasing function that approaches zero as cloud thickness approaches zero.</i>
M2-13	CLDTOT	Total cloud area fraction – <i>The proportion of the sky covered by all the visible clouds, an important influence on downward solar radiation.</i>

M2T1NXLND		2D Land surface variables
M2-14	LAI	<p>Leaf area index</p> <p>– <i>A complex variable that relates the size of plant canopies to canopy density and the angle at which leaves are oriented to one another and to incident light. A dimensionless quality that is often used as an indicator of plant growth rate.</i></p>
M2-15	GRN	<p>Vegetation greenness fraction</p> <p>– <i>The proportion of ground covered by green vegetation. Values range from 0 to 1.</i></p>
M2-16	GWETPROF	<p>Average profile soil wetness</p> <p>– <i>The amount of water and water vapor present in the soil, generally expressed as the proportion of water present in a given volume of soil. Values range from 0 to 1.</i></p>
M2-17	GWETROOT	<p>Root zone soil wetness</p> <p>– <i>The amount of water and water vapor available to plants in the root zone, generally considered to be the upper 200 cm of soil, expressed as the proportion of water present in a given amount of soil. Values range from 0 to 1.</i></p>
M2-18	TSURF	<p>Mean land surface temperature (K)</p> <p>– <i>The radiative temperature of the Earth's land surface, expressed in degrees Kelvin.</i></p>
M2-19	TSAT	<p>Surface temperature of saturated zone (K)</p> <p>– <i>Surface temperature of soil in which all the interstices or voids are filled with groundwater, expressed in degrees Kelvin.</i></p>
M2-20	FRWLT	<p>Fractional wilting area</p> <p>– <i>Proportion of the land surface where the moisture content causes plants to wilt. Values range from 0 to 1.</i></p>
M2-21	QINFIL	<p>Soil water infiltration rate ($[\text{km}/\text{m}^2]/\text{s}$)</p> <p>– <i>A measure of how fast water enters the soil, expressed in mm per second. [1 kg of water spread over a square meter (kg/m^2) = 1 mm]</i></p>
M2-22	GHLAND	<p>Downward heat flux into topsoil layer (W/m^2)</p> <p>– <i>The amount of thermal energy transferred to the soil, which can be affected by such factors as soil and air temperature, soil water content, canopy characteristics, and wind speed, expressed in Watts per square meter.</i></p>

M2-23	WCHANGE	Total land water change per unit time ($\text{[kg/m}^2\text{]}/\text{s}$) – <i>Total rate of movement of water to and from the Earth's surface, expressed in mm per second. [1 kg of water spread over a square meter (kg/m^2) = 1 mm].</i>
M2-24	ECHANGE	Total land energy change per unit time (W/m^2) – <i>Total rate of energy transferred to and from the Earth's surface, expressed in Watts per square meter.</i>
M2-25	PRMC	Total profile soil moisture content (m^3/m^3) – <i>The amount of water present in the soil, expressed as cubic meters of water per cubic meter of soil.</i>
M2-26	RZMC	Root zone soil moisture content (m^3/m^3) – <i>The amount of water in the soil root zone, expressed as cubic meters of water per cubic meter of soil.</i>
M2-27	EVPSOIL	Bare soil evaporation energy flux (W/m^2) – <i>The rate of radiant energy transfer when water evaporates from a saturated land surface, expressed in Watts per square meter.</i>
M2-28	EVPTRNS	Transpiration energy flux (W/m^2) – <i>The amount of energy released as water evaporates at the plant leaf / atmosphere interface, expressed in Watts per square meter.</i>
M2-29	EVPINTR	Interception loss energy flux (W/m^2) – <i>The portion of precipitation that is returned to the atmosphere through evaporation from plant surfaces or absorbed by plants and does not reach the ground, expressed in Watts per square meter.</i>
M2-30	EVLAND	Evaporation from land ($\text{[kg/m}^2\text{]}/\text{s}$) – <i>The rate of moisture transfer from the land surface to the atmosphere, expressed in mm per second. [1 kg of water spread over a square meter (kg/m^2) = 1 mm]. Evapotranspiration is the sum of all processes by which water moves from the land surface to the atmosphere via evaporation (EVLAND, EVPINTR, etc.) and transpiration (EVPTRNS).</i>